Autophagy

Volume 11 - Issue 11 - November 2015

Editor-in-Chief
Daniel J. Klionsky
University of Michigan

Taylor & Francis
Taylor & Francis Group

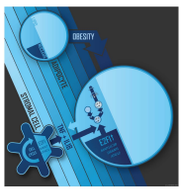

Autophagy

ISSN: 1554-8627 (Print) 1554-8635 (Online) Journal homepage: https://www.tandfonline.com/loi/kaup20

Induction of autophagy increases the proteolytic activity of reservosomes during *Trypanosoma cruzi* metacyclogenesis.

Antonella Denise Losinno, Santiago José Martínez, Carlos Alberto Labriola, Carolina Carrillo & Patricia Silvia Romano

To cite this article: Antonella Denise Losinno, Santiago José Martínez, Carlos Alberto Labriola, Carolina Carrillo & Patricia Silvia Romano (2020): Induction of autophagy increases the proteolytic activity of reservosomes during *Trypanosoma cruzi* metacyclogenesis., Autophagy, DOI: 10.1080/15548627.2020.1720428

To link to this article: https://doi.org/10.1080/15548627.2020.1720428

Accepted author version posted online: 26 Jan 2020.

Publisher: Taylor & Francis & Informa UK Limited, trading as Taylor & Franci

Journal: *Autophagy*

DOI: 10.1080/15548627.2020.1720428

Induction of autophagy increases the proteolytic activity of reservosomes during *Trypanosoma cruzi* metacyclogenesis.

Antonella Denise Losinno[1, 2], Santiago José Martínez[1], Carlos Alberto Labriola[3], Carolina Carrillo[4], Patricia Silvia Romano[1, 2]*

[1] Laboratorio de Biología de *Trypanosoma cruzi* y la célula hospedadora. Instituto de Histología y Embriología (IHEM-CONICET), Mendoza, Argentina.

[2] Facultad de Ciencias Médicas, Universidad Nacional de Cuyo (FCM-UNCUYO), Mendoza, Argentina.

[3] Fundación Instituto Leloir (FIL-CONICET), Buenos Aires, Argentina.

[4] Instituto de Ciencias y Tecnología Dr. César Milstein (ICT—CONICET), Buenos Aires, Argentina.

***Corresponding author**: Patricia S. Romano. Laboratorio de Biología de *Trypanosoma cruzi* y la célula hospedadora. Instituto de Histología y Embriología (IHEM-CONICET), Facultad de Ciencias Médicas, Universidad Nacional de Cuyo, Casilla de Correo 56, Centro Universitario, Parque General San Martín, (5500) Mendoza, ARGENTINA.

Phone. 54-261-4494143 Ext. 7009, Fax: 54-261-4494117

E-mail: promano@fcm.uncu.edu.ar

Running title: Autophagy activates cruzipain during *T. cruzi* metacyclogenesis.

Key words: autophagy, cruzipain, metacyclogenesis, TcAtg8.1, *T. cruzi*.

Abstract

Cruzipain, the major cysteine protease of the pathogenic protozoa *Trypanosoma cruzi*, is an important virulence factor that plays a key role in the parasite nutrition, differentiation and host cell infection. Cruzipain is synthesized as a zymogen, matured, and delivered to reservosomes. These organelles that store proteins and lipids ingested by endocytosis undergo a dramatic decrease in number during the metacyclogenesis of *T. cruzi*. Autophagy is a process that digests the own cell components to supply energy under starvation or different stress situations. This pathway is important during cell growth, differentiation and death. Previously, we showed that the autophagy pathway of *T. cruzi* is induced during metacyclogenesis. This work aimed to evaluate the participation of macroautophagy/autophagy in the distribution and function of reservosomes and cruzipain during this process. We found that parasite starvation promotes the cruzipain delivery to reservosomes. Enhanced autophagy increases acidity and hydrolytic activity in these compartments resulting in cruzipain enzymatic activation and self- processing. Inhibition of autophagy similarly impairs cruzipain traffic and activity than protease inhibitors, whereas mutant parasites that exhibit increased basal autophagy, also display increased cruzipain processing under control conditions. Further experiments showed that autophagy induced cruzipain activation and self-processing promote *T. cruzi* differentiation and host cell infection. These findings highlight the key role of *T. cruzi* autophagy in these processes and reveal a potential new target for Chagas disease therapy.

Abbreviation list: Baf: bafilomycin A_1; CTE: C-terminal extension; Cz: cruzipain; IIF: indirect immunofluorescence; K777: vinyl sulfone with specific Cz inhibitory activity; Prot Inh: broad-spectrum protease inhibitor; Spa1: spautin-1; Wort: wortmannin.

Introduction

Chagas disease, produced by the infection with the protozoan parasite *Trypanosoma cruzi*, is a chronic and silent illness endemic in Latin-American countries. The World Health Organization (WHO) included this pathology among the 20 so-called neglected tropical diseases characterized by the high distribution in the world registered in the last years due to the increased number of infected people, even in non-endemic countries [1]. This scenario and the fact that the current treatment is partially effective highlight the urgent necessity to find new drugs, particularly in the chronic stage, that still does not have a cure. A growing number of drugs with trypanocidal activity are in study nowadays; some of them are even in clinical trials [2]. One validated target for Chagas disease chemotherapy is Cz, the major cysteine protease of *T. cruzi* [3].

Cz, also known as cruzain or GP57/51, belongs to the papain C1 family of cysteine proteases with a specificity intermediate between CTSL (cathepsin L) and CTSB [4]. Natural Cz is a complex of isoforms encoded by a large number of genes arranged in tandems located on 2 to 4 chromosomes. These genes encode the signal peptide, the pro-peptide required for the correct folding of all papain family proteinases, and the mature cruzipain. Mature Cz consists of a catalytic moiety and a 130 amino acid long C-terminal extension (CTE) that is a unique feature of cysteine proteases from trypanosomatids [5]. Most heterogeneities of a mature enzyme are based on the high number of polymorphisms found in the genes encoding the CTE domain. Other differences are present in the carbohydrate composition at the only N-glycosylation site [6]. The CTE domain is eliminated by self-proteolysis, the resultant catalytic domain has kinetic properties similar to those of native cruzipain. While the catalytic domain is sensible to complete self-digestion, the CTE is resistant to proteolysis and can remain as the unique band recognized by a specific anti-cruzipain antibody by western blot [7].

Cz is expressed in all developmental stages of *T. cruzi* and is present in lysosome-like organelles. The highest concentration of Cz is found in the pre-lysosomal organelle of epimastigotes, called the reservosome. In amastigotes, it is preferentially located in the plasma membrane, whereas in trypomastigotes, some isoforms become secreted to the medium [5]. Epimastigotes are highly polarized cells with a single nucleus that separate the cell in the anterior and posterior regions. The Golgi apparatus and the flagellar pocket, the site for endo/exocytosis, are located at the anterior region, whereas reservosomes locate in the posterior region. Similar to late endosomes, reservosomes are organelles generated by the fusion of vesicles from the endocytic and secretory pathways [8]. These organelles, which store proteins and lipids, consume their content and disappear in metacyclogenesis, the parasite differentiation process from epimastigotes to metacyclic trypomastigotes [9]. The biosynthetic secretory pathway delivers Cz to reservosomes. Also, the presence of the pro-peptide is necessary and sufficient for directing Cz from the Golgi complex to the endocytic compartments [10]. Furthermore, compounds that inhibit Cz activity and induce major alterations in the Golgi complex with dilations of peripheral cisternae due to an accumulation of immature Cz [11]. The pro-domain is also an important inhibitor of Cz activity [12]. Although Cz activation is important for Cz trafficking and localization, the precise mechanism that carries out this process is still not fully understood.

Autophagy is a process that works in the degradation of intracellular components by the action of lysosomal enzymes. Multiple physiological and pathological situations require the participation of this vesicular pathway. At basal levels, autophagy operates to remove

long-lived proteins and old or damaged organelles and, thus, produce simple compounds that are then useful in the cell. This process also can be activated under different stress situations such as nutrient starvation, accumulation of unfolded proteins, or even the presence of intracellular microorganisms. Autophagy proteolysis starts with the entrapment of proteins and organelles, then enclosed in a double membrane structure called the autophagosome. After interaction with endocytic (or phagocytic) compartments, autophagosomes fuse with lysosomes to form autolysosomes. By the action of lysosomal enzymes, autolysosomes hydrolyze the trapped materials, and the resulting materials go back to the cytoplasm for recycling.

Autophagy is a highly conserved pathway in eukaryotic cells. Similar groups of genes control this pathway from yeast to mammalian cells. Some of these autophagy-related genes are also found in *T. cruzi* that possess a less complex route [13,14]. Two major kinases regulate autophagy activity. MTOR (mechanistic target of rapamycin kinase) stimulates protein synthesis and cell growth, whereas it strongly inhibits autophagy. Conversely, the class III PtdIns3K complex induces autophagy by promoting the synthesis of PtdIns3P at the phagophore assembly site membranes. Rapamycin, a potent inhibitor of MTOR kinases from different species, including *T. cruzi,* is commonly used as an autophagy inducer [15,16]. In contrast, Wort and other PtdIns3K inhibitors prevent the autophagy response due to a reduction in the autophagosome formation. In mammalian cells, Baf, a proton pump inhibitor that affects the lysosomal function and, therefore, the degradation of autophagy materials, can also inhibit autophagy, yielding an increased number (and size) of autophagosomes that accumulate in the cell [17]. Both Wort and Baf function as autophagy inhibitors in *T. cruzi,* but, in contrast to mammalian cells, Baf treatment affects autophagosome formation [16]. Previous work has demonstrated that acidification of acidocalcisomes is essential for autophagy initiation in *T. brucei* [17]. Although the specific mechanism is still unknown, blocking acidification by Baf seems to have the same effect in *T. cruzi* than in *T. brucei*.

Autophagy is a key process during cellular growth, differentiation, and death. During their life cycle, protozoan parasites undergo morphological and metabolic changes to adapt to different environments and nutritional conditions for the transition from a type of host to another. In this context, autophagy emerges as a crucial process to carry out these transformations. The turnover of glycosomes, the peroxisome-like organelles that compartmentalize the glycolysis in trypanosomatids, carried out with the participation of autophagy plays a key role during *T. brucei* differentiation [18]. Autophagy was also induced during *T. cruzi* metacyclogenesis from the replicative epimastigotes into the infective metacyclic trypomastigotes [14,16]. There are suggestions that the upregulation of autophagy during *T. cruzi* differentiation is responsible for the dramatic reduction of reservosomes observed in metacyclic parasites [13].

Due to the participation of Cz in the parasite differentiation and the infection process, this enzyme is a potential target for drugs to treat Chagas disease. There is evidence that extracellular localization of Cz is related to its role as a virulence factor. By studying the infectivity of different *T. cruzi* strains, previous works demonstrated that there is a correlation between the level of Cz secreted by trypomastigotes and the capacity of the pathogen to invade host cells [19]. Additionally, Cz activates latent TGFB1/TGF-β to trigger TGFB1-mediated events elicited during the *T. cruzi* invasion into the host cell [20]. Furthermore, kinin peptides proteolytically generated by Cz bound to BDKRB1/2 (bradykinin receptor B1/2) enhancing *T. cruzi* invasion, inflammatory responses, and chagasic vasculopathy [21]. *T. cruzi* metacyclogenesis also requires Cz in such a way that parasites overexpressing Cz displayed enhanced ability to undergo metacyclogenesis compared to the control [21]. Chagasin, the endogenous inhibitor of Cz, and other proteolytic inhibitors modulate parasite differentiation and infection processes indicating that proteolytic activity of the enzyme is key to achieve these

biological functions [22]. In this work, we found that the induction of autophagy in *T. cruzi* during metacyclogenesis triggers Cz trafficking on the biosynthetic-secretory pathway to reservosomes. These compartments become more acidic and hydrolytic resulting in an increased enzymatic activity of Cz that promotes parasite differentiation. Inhibition of autophagy impairs Cz transport and activation, similar to treatment with protease inhibitors. Moreover, mutant parasites with high endogenous autophagic activity displayed higher Cz processing. Interestingly, starved trypomastigotes distribute Cz in vesicles located in the cell periphery and display more infectivity than controls; two properties abolished in the presence of autophagy inhibitors. Together, these data point to autophagy as a key process carried out during *T. cruzi* differentiation and host cell infection.

Results

Induction of autophagy increases the cruzipain delivery to reservosomes.

In previous work, we demonstrated *T. cruzi* metacyclogenesis requires autophagy [16]. Following an *in vitro* method of *T. cruzi* differentiation [23], we found a higher autophagic activity in epimastigotes subjected to nutritional stress-induced by TAU medium compared with parasites maintained in control condition [16]. To disclose the possible effect of autophagy in the parasite remodeling occurred during metacyclogenesis, we detected Cz, the classical reservosome marker, to study the localization of these compartments during this process. After 2 h of autophagy induction (1st stage of metacyclogenesis), we fixed parasites, and detected Cz by IIF using a specific polyclonal antibody generated in the rabbit, which recognizes the precursors and the mature form of the enzyme and even the self-proteolysis products [24,25]. By confocal microscopy, we found Cz in compartments distributed at different regions of the cell body in control (BHT) or TAU media (**Fig. 1A**). Considering the spatial position of nucleus (stained with Hoechst), and the region where the flagellum emerges to the cell surface, we classified the Cz distribution as anterior, posterior or homogenous, when we located the compartments between the nucleus and the origin of flagellum; between the nucleus and the opposite side without flagellum; or in both anterior and posterior regions of epimastigotes, respectively (**Fig. 1B**, scheme). Quantification studies showed that, in contrast to parasites under the control medium, epimastigotes incubated in TAU medium displayed Cz preferentially in the posterior region, which is the usual location for reservosomes [11,26] (**Fig. 1B**). To confirm the Cz localization in reservosomes, we performed an endocytosis assay of small fluorescent beads as previously described by Vidal and colleagues, taking into account that reservosomes are the last compartments of the endocytic pathway, where macromolecules are stored [27]. The colocalization of Cz and beads significantly increased under TAU medium compared to the control condition (**Fig. 1C and D**). In addition, the localization of autophagosomes was studied during this process by detection of the Tc Atg8.1 protein by IIF. As shown in **Fig. 1E and F**, Cz and Atg8.1 colocalized in compartments located at the posterior region of epimastigotes in BHT medium. This colocalization significantly increased in the TAU medium when parasites achieved maximal autophagic activity and distributed autophagosomes in the entire parasite body.

In agreement with previous works, the distribution of Cz in the anterior and posterior regions of parasites in control conditions denotes the normal transport of this enzyme through the biosynthetic-secretory pathway of *T. cruzi*, from the endoplasmic reticulum and Golgi apparatus, located in the anterior side of epimastigotes, to reservosomes in the posterior side [11,26,28]. In contrast, under TAU treatment, Cz is mainly located at the posterior side, indicating that all Cz synthesized up to that moment was delivered to reservosomes. To check the effect of autophagy on Cz trafficking, we treated parasites with TAU medium and the addition of Wort or Baf, two compounds that abrogate the *T. cruzi* autophagy response [16]. As is shown in **Fig. 2A**, Cz-containing compartments

distributed in the whole cell body when we added these inhibitors to the TAU medium. Interestingly, inhibition of the hydrolytic activity by the addition of (Prot Inh produced the same effect of autophagy inhibitors. The percentage of parasites with different localizations was quantified for each condition and confirmed that inhibition of autophagy or protease activity impaired Cz traffic to reservosomes, remaining the enzyme in compartments localized at anterior and posterior sides of the *T. cruzi* cell (**Fig. 2B**).

Induction of autophagy maturates reservosomes into lysosomes.

Next, we studied the acidic and hydrolytic properties of reservosomes containing Cz after autophagy induction. We used LysoSensor dye to evaluate the acidity of these compartments when we stimulated nutritional stress in comparison with optimal nutritional conditions. By confocal microscopy, we observed that reservosomes displayed very low colocalization with LysoSensor under the control medium, but it significantly increased after 2 h of TAU treatment (**Fig. 3A and B**). In addition, acidity also increased in reservosomes when we induced autophagy, given the high degree of LysoSensor fluorescent intensity detected in the Cz-positive compartments from parasites exposed to differentiation (**Fig. 3C**). Then, we analyzed the hydrolytic capacity of reservosomes by using the self-quenched albumin (DQ-BSA) reactive. The colocalization of Cz-positive compartments with DQ-BSA was low (around 30%) in the control condition. In contrast, reservosomes displayed high colocalization (more than 90%) with this marker in the TAU medium (**Fig. 3D and E**). Together, these findings suggest that reservosomes become more acidic and hydrolytic upon autophagy induction. Further studies performed at later times of differentiation (72 h) confirmed an increment in the triple colocalization (Mander's coefficient > 0.5) between Cz-, Atg8.1- and DQ-BSA-positive compartments, during autophagy induction (**Fig. 4**).

***Inhibition of autophagy prevents cruzipain degradation during the metacyclogenesis of* T. cruzi.**

Due to Cz is synthesized as a zymogen and its mature form displays autocatalytic activity, we decided to study the possible modifications of Cz during the induction of autophagy by western blot. As shown in **Fig. 5**, in the first stage of metacyclogenesis, Cz was presented as a unique band of 50 kDa, which corresponds to the mature form in both control and TAU conditions (**Fig. 5A, 2 h**). At later times (48 and 72 h), while the control maintained the same band of mature Cz, under TAU condition, two additional bands of 37 and 25 kDa were detected (**Fig. 5A, 48 and 72 h**). It is worth mentioning that an equal amount of proteins was running in each lane, even when the total amount of protein reduced in the samples subjected to TAU treatment due to the absence of parasite replication [29]. In agreement with previous reports [7], these new bands correspond to fragments of processed Cz: a product of partially degraded Cz and the CTE, which is resistant to self-proteolysis, respectively. Next, we decided to study the effect of the inhibition of autophagy on the processing of Cz. Interestingly, when the autophagy inhibitors were present only at the first 2 h, they did not prevent the Cz degradation (**Fig. 5B, Baf and Wort lanes**). However, we prevented Cz processing when we maintained the inhibitors during the total time of differentiation (**Fig. 5C, Baf and Wort lanes**). Notably, the treatment of parasites with protease inhibitors prevented the Cz processing at both times (**Fig. 5B and C, Prot Inh lane**), indicating that in contrast to autophagy inhibition, the effect of protease inhibitors was maintained through the time. In addition, to assess if Cz degradation occurred by the action of another protease or if this feature was a consequence of the self-processing, we treated parasites with K777, a vinyl sulfone drug that acts as a specific Cz inhibitor [30] during the total time of differentiation, and we noted that we inhibited Cz degradation in this

condition (**Fig. 5D**). Because of wortmannin is a general PtdIns3K inhibitor, we decided to confirm the effect of autophagy inhibition on Cz distribution and molecular forms by the use of Spa1, a specific autophagy inhibitor that promotes the degradation of the BECN1 subunit of PtdIns3K complexes [31]. Detection of Cz by IIF and later microscopy analysis showed that Cz-positive compartments localized in the whole parasite body under TAU treatment in the presence of Spa1 (**Fig. S1A**). As expected, similar to Wort, we observed Spa1 inhibition of Cz processing by western blot when this inhibitor was maintained during the total time of metacyclogenesis, in which we detected only the mature form of Cz (50 KDa) (**Fig. S1B and C**). Overall, these data confirmed the effect of autophagy inhibition on Cz delivery to reservosomes and processing and highlighted the participation of autophagy in this process.

Enzymatic activity of Cz was then studied at 72 h by two different methods. Firstly, we made a zymography, separating protein extracts obtained from parasites under different treatments on gelatin-SDS-PAGE. Zymograms showed that, except for protease inhibitors and K777 treatments that completely inhibited Cz activity, the rest of the treatments displayed some proteolytic activity. Under optimal nutritional conditions (BHT), there was high enzymatic activity following the absence of Cz processing, while TAU treatment caused a decrease in activity since, in this condition, Cz became degraded (**Fig. 5A and 6A**). Inhibition of autophagy by Wort recovered Cz activity compared to TAU condition. This effect did not occur under Baf treatment, possibly due to the way of action of this compound on the parasite (**Fig. 6A**). In addition, we assayed Cz activity with a specific chromogenic substrate reaction (**Fig. 6B**) that showed similar results than zymography, with statistical significance. Further studies at 24 h of differentiation confirmed that Cz was still not processed at this time (**Fig. S2A**) and displayed more activity in TAU compared to BHT (**Fig. S2B and C**). Together, these data indicate that induction of autophagy promotes the Cz activation at early times of differentiation (24 h) followed by Cz self-proteolysis at later times (48 and 72 h).

Effect of cruzipain processing on metacyclogenesis.

As previously demonstrated, Cz is an important virulence factor required for *T. cruzi* differentiation [21,22]. In the above results, we showed that induction of autophagy during metacyclogenesis transports Cz from the anterior region of the parasite, where the pre-pro-enzyme is synthesized, to the reservosomes located in the posterior region. Late acidification of reservosomes is a key process to induce Cz activation and self-processing. Next, we studied the performance of metacyclogenesis according to the presence of autophagy or proteases inhibitors. Parasites were subjected to differentiation for 72 h and then classified as epimastigote, metacyclic trypomastigote (MT), or intermediate forms (IF), according to the relative position of the kinetoplast, nucleus and flagellum origin (**Fig. 7A**). Our results showed that under TAU treatment, metacyclogenesis was more efficient compared to the control condition, given the increment observed in the percentage of MT forms (**Fig. 7B, TAU vs. BHT**). Inhibition of autophagic or proteolytic activity significantly reduced the number of parasites suffering complete or incomplete differentiation (MT and IF) (**Fig. 7B, Wort, Baf or Prot Inh**). These results are in agreement with those obtained in the presence of the K777 drug (**Fig. 7C**) and emphasize the fact that the induction of autophagy and the degradation of Cz are two related processes required during the metacyclogenesis of *T. cruzi.*

In previous work, we demonstrated that the *T. cruzi* ODC mutant strain (Y-GFP-ODC) that overexpresses the ODC enzyme and possesses high levels of intracellular polyamines (PA), displayed higher metacyclogenesis capacity compared to the control wild type strain [32]. Recently we demonstrated that this mutant had increased basal autophagic activity [16]. To assess if the high autophagy and the metacyclogenesis

efficiency are related to Cz processing, we studied the localization and molecular forms of Cz in epimastigotes from *T. cruzi* ODC mutant strain during the first stage of differentiation. Interestingly, the localization of Cz in this strain was predominantly posterior in both control (SDM) and TAU medium (**Fig. 8A and B**). Moreover, in contrast to the *T. cruzi* Y-GFP strain, in the mutant ODC strain, Cz was already processed at 2 h of differentiation under control conditions (**Fig. 8C**). These data confirmed that during metacyclogenesis, autophagy induction is crucial to activating Cz that drives the parasite differentiation to generate the infectious forms of *T. cruzi.*

Participation of cruzipain during the* T. cruzi *infection process.

It has been shown that Cz has an important role in *T. cruzi* host cell infection [33]. Then, we studied the localization of Cz in trypomastigotes maintained in control medium (DMEM) in the absence or presence of K777, or PBS in absence or presence of inhibitors of autophagy, of protease activity or Cz during 2 h. In agreement with previously published works [33–35], in trypomastigotes maintained in control conditions with or without K777, Cz was mainly concentrated in compartments located between the kinetoplast and the nucleus (**Fig. 9A**). Interestingly, in starved trypomastigotes (PBS), Cz adopted a pattern of distribution in dots, which were not only between the nucleus and the kinetoplast but also was close to the membrane and throughout the parasite body (**Fig. 9A**). On the other hand, in the presence of autophagy or hydrolytic inhibitors, Cz retained the distribution observed in trypomastigotes under control medium, and we observed the same location under the K777 treatment (**Fig. 9A**). It has been suggested that Cz peripheral localization is crucial to produce the exocytosis of vesicles containing Cz during host cell invasion [35]. Therefore, to study the possible effect of autophagy modulation in host cell infection, we pretreated trypomastigotes with PBS or with inhibitors of autophagy or proteases for 2 h and then incubated with host cells for 6 h in control conditions to follow the infection process (see **Fig. 9B** for a schematic representation). As shown in the **Fig. 9C**, starvation of trypomastigotes with PBS before exposition to host cells significantly increased the infection. On the other hand, inhibition of autophagy by pretreatment with autophagy or protease inhibitors decreased the infection rate. Reduced infectivity was also observed when trypomastigotes were pretreated with a K777 drug. Together, these data confirmed the effect of autophagy on the Cz localization and *T. cruzi* infection process.

Discussion

One of the key processes in the mammalian infection by *T. cruzi* is the parasite entry into the host cell. To achieve this, *T. cruzi* employs several soluble and membrane-bound molecules that are involved in invasion, and other processes such as inflammation and immune modulation [33]. Cz, the major cysteine proteinase of *T. cruzi,* is required for parasite differentiation to the infective form and is released by trypomastigotes during the invasion, which makes it a key virulence factor and a specific and validated target against *T. cruzi* infection in Chagas disease [4,19]. Therefore, the knowledge about the intracellular transport and activation of Cz in this protozoan parasite is central in the field of drug discovery to find new and more specific compounds that impair the normal Cz function.

It has been demonstrated that Cz presents specific subcellular distribution for each developmental stage of *T. cruzi*, which could imply that this enzyme plays different roles during the life cycle of the parasite. This understanding would allow its adaptation to the environment of each particular host [21]. Under normal nutritional conditions, Cz is in compartments located at the anterior, posterior, or both regions of epimastigotes. This distribution revealed the enzyme traffic on the biosynthetic secretory pathway from the endoplasmic reticulum and Golgi complex, located from the anterior side of the parasite

nuclei to reservosomes at the posterior side [11]. Otherwise, in trypomastigotes, the infective form of *T. cruzi*, Cz is found in organelles localized between the kinetoplast and the nucleus, in addition to its presence in vesicles that are distributed near the flagellar pocket and close to the plasma membrane, ready to be delivered from the parasite by exocytosis [35–37]. In this work, we observed that in epimastigotes starved during 2 h in TAU medium (first period of metacyclogenesis), Cz is mainly concentrated in reservosomes, suggesting that Cz synthesis is interrupted and the total content of this enzyme is transported to these compartments. The presence of endocytic markers in the Cz-positive compartments evidences the previously demonstrated fusion events between the endocytic and secretory pathways in the biogenesis of reservosomes [8]. In contrast, in the presence of autophagy inhibitors, Wort, Baf, or Spa1, Cz remained at both anterior and posterior compartments similar to the control medium. Interestingly, inhibition of protease activity with a broad-spectrum inhibitor showed a similar pattern of Cz distribution than autophagy inhibitors. These data suggest that both hydrolytic activity and autophagy induced by starvation are participating in the Cz trafficking to reservosomes. The higher level of colocalization between Cz and TcAtg8.1, the specific marker of *T. cruzi* autophagosomes, further confirms the participation of autophagy in this process.

The acidity and hydrolytic activity also increased in Cz-positive compartments at the first stage of metacyclogenesis. Because acid hydrolases are resident proteins of reservosomes, this could indicate an autophagy-dependent increment of protons into these compartments, which increase the activity of hydrolases and allow the maturation of reservosomes into lysosomes. The normal transport of Cz appears to require acidification and the activation of Cz. Previous works demonstrated that the treatment of parasites with a specific Cz inhibitor accumulates inactive Cz in the Golgi cisternae instead of reservosomes, leading to parasite death [11,26]. Acidocalcisomes, other specific compartments of *T. cruzi*, are lysosome-related organelles (LROs) with high acidity and content of calcium and phosphate ions [38]. It has been demonstrated that acidification of acidocalcisomes followed by starvation is crucial to induce autophagosome formation in *T. brucei* [17]. Treatment with Baf or other proton pump inhibitors strongly decreased the number of autophagic compartments. Because this effect is restricted to acidocalcisomes, the authors propose membranes derived from these organelles form the autophagosome. In this sense, and taking into account that Baf also inhibited autophagosome formation in *T. cruzi* [16], we hypothesized that Baf-sensitive proton pumps required for acidocalcisome acidification may be included in the autophagosome membrane during the autophagosome formation and delivered to reservosomes through the autophagy pathway. In support of this, we showed that colocalization between Cz, TcAtg8.1, and DQ-BSA significantly increased under starvation. Furthermore, previous work showed a typical autophagosomal content inside reservosomes by electron microscopy [13]. Together, these data are in agreement with the hypothesis that nutritional stress triggers the acidification of the luminal content of reservosomes by the fusion of autophagosomes, and the activation of the enzymes contained inside. It is well known that the lysosomal compartment expands in starved cells. Degradation of materials in autolysosomes are crucial to providing substrates for energy supply at this condition. During *T. cruzi* metacyclogenesis, epimastigotes at the exponential phase switch from glucose to amino acid consumption [29]. Therefore, the maturation of reservosomes into lysosomes will allow the amino acid and energy supply required to ensure parasites' survival and differentiation.

In agreement with the above data, we observed that the induction of autophagy increases Cz activity at early times, followed by self-proteolysis at later times of metacyclogenesis. This Cz processing starts after 24 h of metacyclogenesis by the degradation of Cz mature form which yields intermediate enzymatic fragments and a C-terminal extension that is resistant to proteolysis [7]. Moreover, the inhibition of

autophagic and proteolytic activity during the complete differentiation period abrogates the Cz self-processing. Previous work demonstrated that Cz could degrade itself, producing a complex mixture of peptides and a glycosylated fragment with an apparent molecular weight of 25 kDa [39]. The absence of these Cz fragments in starved epimastigotes under K777 treatment, the specific inhibitor of Cz [40], confirms that the processing detected by us is due to the self-activity of Cz. As a consequence of this degradation, the *in vitro* activity of Cz (measured after the differentiation process) displayed a significant decrease when autophagy is induced under TAU treatment, whereas inhibition of autophagy by treatment with Wort restored – at least partially – the Cz activity. As expected, Cz remains inactive in the presence of general or specific protease inhibitors, although it is displayed as a unique band corresponding to the mature form by western blot. The effect of Baf seems to be similar to the enzyme inhibitors. Under this treatment, the enzyme is not active, and it is displayed as the mature form by western blot. Because Baf is a vacuolar-type H^+-ATPase inhibitor [17], this result indicates that acidification of reservosomes is required for enzyme activation. In other words, higher reductions of pH in reservosomes induced under restricted nutritional conditions result in the optimal conditions for Cz enzymatic activity and self-processing. These data highlight the subtle regulation of Cz activity that could be caused by multiple factors such as pH, nutritional conditions, and presence of inhibitors [11].

Due to Cz activity in epimastigotes is 10-fold higher than other parasite forms [25,41,42], we hypothesized that Cz activation is a required event to drive metacyclogenesis. In agreement with this, our work shows a significant reduction in the percentage of trypomastigotes obtained when we performed metacyclogenesis in the presence of K777. We also obtained low percentages of metacyclic trypomastigotes under treatment with protease inhibitors and in conditions that inhibit autophagy as we previously demonstrated [16]. In agreement with these data, Tomas A. M. and co-workers demonstrated that overexpression of Cz is associated with enhanced metacyclogenesis [21]. The requirement of Cz activation during metacyclogenesis is also illustrated in the *T. cruzi* Y-ODC strain. Previous works from our laboratory demonstrated the higher ability of this mutant to differentiate from epimastigotes to trypomastigotes [32] and also the increased basal autophagic activity due to the higher levels of polyamines synthesized in these parasites [16]. Here, we showed that the Y-ODC strain displayed Cz in compartments located at the posterior region of the parasites in both control or TAU media. Furthermore, the presence of processed forms of Cz by western blot at control conditions infers a high activity of this enzyme. Together these data demonstrate that the increased autophagy activity of this mutant favors the Cz activation and, as a result of this, causes higher differentiation rates.

It is important to note that Cz self-processing is a late event in metacyclogenesis. At earlier times of 24 h, our data show an increase in the Cz activity in starved epimastigotes. The hydrolysis of proteins stored in reservosomes by Cz and also the degradation of lipids is, as explained above, two important reactions that supply energy to drive the differentiation process. Besides its energetic functions, protein degradation could also be important as a source of L-proline, L-glutamine, and L-asparagine, three amino acids required for *T. cruzi* differentiation [23].

Changes in Cz localization in trypomastigotes under autophagy induction are also important for *T. cruzi* infectivity. We observed a different distribution of Cz compartments when we exposed trypomastigotes to starvation conditions compared to control. Peripheral localization of Cz-positive compartments predominantly displayed under starvation may favor the exocytosis of these vesicles during host cell invasion. The major infectivity displayed by pre-starved trypomastigotes confirms the beneficial effect

of autophagy induction for *T. cruzi* infection, whereas the presence of autophagy or proteases inhibitors abolished this effect. Cz is an important virulence factor during *T. cruzi* infection because a decrease in the expression of Cz and trans-sialidase family protein contributes to the loss of *T. cruzi* infectivity *in vivo* [43]. On the other hand, trypomastigotes overexpressing chagasin, a natural inhibitor of Cz, displayed less infectivity *in vitro* than wild type parasites due to lower activity of membrane-associated Cz. However, membranes isolated from wild type trypomastigotes restored the infectivity of these mutant parasites [22]. It is important to note that, in contrast to other proteases, Cz can function in a wide range of pH, being active at the acidic environment of reservosomes and also at the neutral pH of the host extracellular space [44]. This characteristic explains the participation of Cz in biological processes as different as parasite differentiation and host cell infection. In this work, we demonstrated that autophagy participates in the Cz redistribution towards the cell periphery, a crucial event during host cell infection. In agreement with these results, other authors demonstrated that autophagy vesicles were distributed to the cell periphery and secreted its content after autophagy induction [45]. It is possible that in contrast to the role of autophagy in the activation of Cz during the metacyclogenesis of epimastigotes, in trypomastigotes, autophagy participates in the exocytosis of Cz having a role in the infectivity of *T. cruzi*. More studies will be necessary to confirm this function.

In summary, in replicating epimastigotes, Cz is continuously synthesized and transported from ER to Golgi cisternae and further to reservosomes where its hydrolytic activity is displayed (**Fig. 10, Epimastigote**). After metacyclogenesis initiation, Cz synthesis is interrupted, and all Cz content delivered to reservosomes. Autophagy vesicles generated from acidocalcisomes fused with reservosomes and contribute to increasing the acidic pH and the hydrolytic activity of Cz (**Fig. 10, Intermediate form**). In metacyclic trypomastigotes, we observed Cz in compartments located at the posterior side of trypomastigotes between the kinetoplast and the nucleus. We could also observe this enzyme in small vesicles distributed close to the plasma membrane in the whole parasite body, especially when we subjected the parasites to starvation (**Fig. 10, Metacyclic trypomastigote**). In conclusion, in this work, we contributed with the knowledge of the activation and processing of the mature Cz under the induction of autophagy and demonstrated the role of this process in two key stages of the *T. cruzi* biological cycle, such as differentiation from epimastigote to trypomastigote and host cell infection. Therefore, *T. cruzi* autophagy arises as a good target for drug discovery to improve Chagas disease treatment in the future.

Materials and Methods

Media.

TAU medium was prepared with 190 mM NaCl (Biopack, 20000164600), 17 mM KCl (Biopack, 2000163100), 2 mM $MgCl_2$ (Biopack, 2000962000), 2 mM $CaCl_2$ (Biopack, 2000169100), 8 mM sodium phosphate buffer (pH 6 to 6.8). Modified TAU medium (TAU-AAG) was prepared with TAU medium supplemented with 50 mM sodium glutamate (Sigma, 49621), 10 mM L-proline (Sigma, P0380), 2 mM sodium aspartate (Sigma, A6683), 10 mM glucose (Sigma, D9434). Diamond medium contains 6.25 g/L tryptose (Sigma, 70937), 6.25 g/L tryptone (Sigma, T7293), 6.25 g/L yeast extract (Sigma, Y1625), 7.16 g/L KH_2PO_4 (Biopack, 2000963500) (pH 7.2) and 6.66 mM hemin (Calbiochem, 37415GM) prepared in 3 mL 1N NaOH and 20 mL 1 M Tris HCl (Sigma-Aldrich, 10812846001), pH 6.8. BHT medium was prepared with 33 g/L Brain heart infusion broth (Britania), 3 g/L tryptose, 0.4 g/L KCl, 0.3 g/L glucose and 3.2 g/L Na_2HPO_4 (Biopack, 2000979000). SDM79 medium, which contains only traces of polyamines, was prepared with 8.4 g/L 199 TC 45 medium (Sigma, M3769), 8 mL/L MEM amino acids 50x (Gibco, 11130051), s/c L-glutamine (Calbiochem, 3520), 6 mL/L

MEM Non-essential amino acids 100x (Gibco, 11140050), 1 g/L glucose, 8 g/L HEPES (Merck, 391338), 5 g/L MOPS (Merck, 475898), 2 g/L $NaHCO_3$ (Biopack,2000163600), 100 mg/L sodium pyruvate (Sigma, 792500), 200 mg/L L-alanine (Biopack, 2000969900), 100 mg/L L-arginine (Sigma, A5006), 300 mg/L L-glutamine (Sigma, G3126), 70 mg/L L-methionine (Sigma, M9625), 80 mg/L L-phenylalanine (Sigma, P2126), 600 mg/L L-proline (Sigma, P0380), 60 mg/L L-serine (Sigma, S4500), 160 mg/L L- taurine (Sigma, T-0625), 350 mg/L L-threonine (Sigma, T8625), 100 mg/L L-tyrosine (Sigma, T3754), 10 mg/L adenosine (Sigma, A4036), 10 mg/L guanosine (Sigma, G6264), 50 mg/L glucosamine-HCl (Sigma, 1294207), 4 mg/L folic acid (Sigma, F7876), pH 7.3.

***Parasites*.**

Epimastigotes of Y wild type (Y-WT) and Y-GFP (expressing TcH2b histone fused to GFP[46]) strains were cultured in BHT medium with 10% fetal bovine serum at 28˚C. Y-GFP-ODC [32] strain (mutant co-expressing GFP and the ornithine decarboxylase gene [ODC], AN Y08233.1) was maintained in the semisynthetic medium SDM79, to be selected by auxotrophy at 28˚C. All cultures contained 20 mg/L hemin (Calbiochem, 3741), 10% inactivated fetal bovine serum (Gibco, 10082147), 250 µg/mL geneticin (Gibco, 10131035) for GFP selection, 100 mg/mL streptomycin (Gibco, 15140122) and 100 U/mL penicillin (Gibco, 15140122). Stationary phase parasites (5×10^7 cells/mL) were used in all experiments.

T. cruzi *differentiation protocol.*

To induce *T. cruzi* metacyclogenesis, we performed a previously published *in vitro* protocol [16]. Briefly, epimastigotes of *T. cruzi* Y-WT, Y-GFP or the mutant Y-GFP-ODC strains were collected by centrifugation at 2000 *g* for 10 min and suspended at 5×10^8 cells/mL in TAU medium to induce nutritional stress. After 2 h at 37°C (1^{st} stage of metacyclogenesis), parasite samples were processed for microscopy or molecular studies. Similar procedures were conducted in control parasites maintained in BHT or SDM79 medium at 28°C. In the complete differentiation process, after the first 2 h, parasites were diluted 100 times in TAU-AAG or control media as appropriate and maintained at 28°C for 72 h (2^{nd} stage of metacyclogenesis). After this period, differentiated parasites (MT) were used for infection assays (see below), processed for microscopy or molecular studies.
In the indicated cases, different drugs were added to the maintenance medium only in the first stage or in the complete metacyclogenesis process. Wortmannin (Wort, 100 nM; Sigma, W1628), bafilomycin A_1 (Baf, 100 nM, Sigma, B1793) or Spautin-1 (Spa1, 100 nM) were used as autophagy inhibitors, while a cocktail containing pepstatin A, leupeptin and E-64 (Sigma, P2714) was used as a protease inhibitor (Prot Inh). For specific cruzipain inhibition, 10 µM K777 (generously given by Paul Novick and Sara Trosin, Stanford University, USA), was added to the maintenance medium.

***Endocytosis assay associated with metacyclogenesis*.**

Epimastigotes from Y-WT strain were collected by centrifugation at 1500 g for 10 min, washed twice in phosphate-buffered saline (PBS; 10 mM sodium phosphate buffer pH 7·2 plus 9% [w/v] NaCl), and incubated in BHT medium containing 40 nm FluoSpheres carboxylate-modified microspheres (580/605, Invitrogen, F8793) for 30 min at 28°C. Subsequently, the cells were washed twice in BHT medium and then incubated in BHT medium containing 10% fetal bovine serum for 1 h to accumulate the tracer in reservosomes [47]. These parasites were called preloaded epimastigotes. After 1 h, the preloaded epimastigotes were washed and metacyclogenesis was induced in TAU

medium in the absence of drugs, as indicated above. Samples were collected for microscopy after 2 h after the initiation of the metacyclogenesis assay.

***Infection assays*.**

Trypomastigotes from the Y-WT strain were preincubated in DMEM medium (in absence or presence of the specific Cz inhibitor K777) or in PBS in the absence or presence of autophagy inhibitors (Bafilomycin and Wortmannin) or protease inhibitors (K777 or the cocktail containing broad-spectrum protease inhibitors). After 2 h, trypomastigotes were washed with DMEM medium or PBS as appropriate and placed on monolayers of Vero cells (ABAC-Asociación Banco Argentino de Células) for 6 h at 37°C. After 3 washes with PBS, to remove non-internalized parasites, cells were fixed with 4% paraformaldehyde for 15 min at room temperature, incubated with 50 mM NH_4Cl in PBS and rinsed with 0.05% saponin, 0.2% BSA (Sigma, B2064) in PBS for the immunofluorescence technique. To facilitate visualization, cellular actin was stained with rhodamine-conjugated phalloidin (Invitrogen, R415) for 1 h at 37°C in a humid chamber. Parasites were stained with anti-*Trypanosoma cruzi* serum developed in infected rabbits (1:250) that was detected with Cy3-conjugated antirabbit IgG antibodies (1:200 dilutions, Jackson, 111165003). Cells were also treated with Hoechst (Invitrogen, H1399) for DNA staining, mounted onto glass slides with Mowiol and analyzed with an Olympus Confocal Microscope FV1000-EVA (Olympus), with the FV10-ASW (version 01.07.00.16) software.

Determination of the metacyclogenesis performance.

To distinguish *T. cruzi* developmental stages, Hoechst staining and phase contrast was used to identify the nucleus/kinetoplast and flagellum position. Based on parasite morphology, the relative number of epimastigotes, intermediate forms, and metacyclic forms were estimated in each sample obtained from metacyclogenesis assay, according to Ferreira *et al.* (2008) [47]. Epimastigote forms contain a spherical nucleus with a flagellum protruding from the anterior position of the cell body near to the disk-shaped kinetoplast. Intermediate forms have a somewhat elongated nucleus with the kinetoplast varying in position relative to the nucleus, either anterior, at the middle or posterior. Metacyclic trypomastigotes have a fully elongated nucleus with a round kinetoplast at the posterior end of the parasite.

DQ-BSA labeling.

DQ-BSA red and green are compounds that emit red or green fluorescence when BSA is hydrolyzed into small peptides in lysosomes, thus identifying degradative compartments. Epimastigotes from the Y-WT strain were subjected to the first period of metacyclogenesis in TAU or BHT medium for 2 h at 37°C. Thirty min before the end of incubation, 10 µg/mL unquenched BSA (DQ red BSA or DQ green BSA; Invitrogen, D12051 or D12050, respectively) was added to samples. At the end of the first period or the second stage of metacyclogenesis, parasites were centrifuged, washed 3 times with PBS and fixed with paraformaldehyde. Subsequently, samples were processed for immunostaining assay.

Monitoring the acidification of* T. cruzi *compartments.

The LysoSensor™ dye is an acidotropic probe that accumulates in acidic organelles as the result of protonation. This pH-dependent protonation also releases the fluorescence quenching of the dye by its weak base side chain, resulting in increased fluorescence intensity. Epimastigotes from the Y-WT strain were subjected to the first period of metacyclogenesis as previously indicated. Thirty min before the end of incubation, 1 µM

LysoSensor™ Green DND-189 (Invitrogen, L7535) was added to samples. After that, parasites were centrifuged, washed three times with PBS and fixed with paraformaldehyde. Subsequently, samples were processed for immunostaining assay.

Immunostaining.

Parasites fixed with 4% paraformaldehyde, were washed 3 times for 10 min with PBS, incubated in 50 mM NH_4Cl in PBS 30 min, rinsed 3 times for 10 min with 0.05% saponin, 0.2% BSA in PBS (wash solution), and incubated overnight at 4°C with primary antibodies. The antibodies (Abs) used were a monoclonal Ab against TcAtg8.1 protein (1:500 dilution), and a polyclonal Ab against cruzipain protein [24,25] (1:400 dilution), generously given by Dr. Vanina Alvarez (IIB-INTECH UNSAM-CONICET) and Dr. Carlos Labriola (INSTITUTO LELOIR-CONICET) respectively. The samples incubated with Ab against TcAtg8.1 were rinsed with wash solution (3 times for 10 min) and developed with Cy3-conjugated antirabbit IgG Ab (1:200 dilution, Jackson, 111165003). In the same way, samples incubated with Ab against cruzipain were rinsed with wash solution (3 times for 10 min) and developed with Alexa 488-conjugated anti-rabbit IgG Ab (1:200 dilution, Jackson, 711545152) and then rinsed with wash solution. Nuclear and kinetoplast DNA were stained with 2 mg/mL Hoechst 33342 (Invitrogen). Distribution of Cz-containing compartments was classified in anterior, posterior or homogeneous according to the position of Cz signal related to nuclei or, alternatively, related to the free end of the parasite. As shown in the scheme of **Fig. 1B**, the anterior region is the side where emerges the free end of flagellum while the contrary side, from the nucleus to the parasite end without a flagellum, is the posterior region.
For double staining assays (Atg8.1 and cruzipain), parasites were incubated with cruzipain Ab, secondary Ab, cruzipain Ab again (to block the free Fab regions of the secondary Ab), rinsed with wash solution and finally incubated with TcAtg8.1 Ab followed by its secondary Ab. The immunostaining preparations were embedded in PBS, coverslipped, and examined in a confocal microscope (Olympus, FV 1000, Japan) with a Paplon 60x lens. Appropriate negative controls were included to ensure that the staining observed was specific.

Quantitative Colocalization Analysis.

The colocalization analysis was made using the JACoP plugin for Image J software (NIH) according to Bolte and Cordelieres [48]. Images of 50 parasites per condition were studied. The colocalization analysis was made using Mander´s correlation coefficients (MCC). The MCC is based on the Pearson coefficient (PCC), with average intensity values being taken out of a mathematical expression [48]. Two coefficients were obtained, MCC-M1 and MCC-M2 that describe the fraction of cruzipain overlap with TcAtg8.1, DQ-BSA or fluorospheres as appropriate; and the fraction of these markers overlap with cruzipain, respectively. These coefficients adopt values that vary from 0 to 1, corresponding to non-overlapping images or complete colocalization, respectively. In this study, we emphasize the MCC-M1 coefficient to evaluate the degree of relationship between cruzipain and the different markers. Data were expressed as percentages.

Western blot assay.

Parasites from Y-WT or the mutant Y-GFP-ODC strains (30 x 10^6 cells) were collected for western blot assay at 2 or 72 h after starting the metacyclogenesis assay. Samples were collected by centrifugation at 2000 *g* for 15 min and lysed with 25 mM Tris-HCl, pH 7.5; 100 mM NaCl; and 1% (v:v) Nonidet P-40 (NP-40; Sigma, 74385). Protease inhibitors (cocktail) were added immediately before lysis. The samples were centrifuged at 14,000 g for 10 min to remove debris. Protein concentration in the lysates was measured via micro bicinchoninic acid assay (Pierce Thermo Scientific, 23225) following

the manufacturer's protocol to ensure the equal amount of protein per condition (data not shown). Samples were resuspended in sample buffer and cracked for 10 min at 95°C. Protein extracts were separated on 10% SDS-PAGE and transferred to nitrocellulose membranes (Amersham, 10600003). The membranes were blocked for 1 h at room temperature with a solution containing 5% non-fat milk and 0.05% Tween 80 in PBS, washed twice with 0.05% Tween 80 (Sigma, P8192) in PBS and incubated with the primary antibody against cruzipain (1:1000 dilution) overnight at 4°C. Membranes were also incubated with a primary antibody against the heat shock protein family A (Hsp70) member 5 (HSPA5/BiP), a protein of 70 kDa resident in the ER used as a loading control [49] (1:1000 dilution), generously given by Dr. Carlos Labriola (INSTITUTO LELOIR-CONICET). Finally, the membranes were washed with 0.05% Tween 80 in PBS and incubated with a peroxidase-conjugated anti-rabbit secondary antibody (1:10,000 dilution; Jackson, 111035003) for 1 h at 37°C. Detection was accomplished with a chemiluminescence system from Millipore (WBKLS0500) on a Luminescent Image Analyzer LAS-4000 (Fujifilm, Tokyo, Japan).

Zimography.

Parasites from the Y-WT strain were collected 72 h after starting the metacyclogenesis assay. Samples were centrifugated at 2000 *g* for 15 min and lysed with 25 mM Tris-HCl, pH 7.5; 100 mM NaCl; and 1% (v:v) NP-40. Protease inhibitors (cocktail) were added immediately before lysis. The samples were centrifuged at 14,000 g for 10 min to remove debris. Protein concentration in the lysates was measured via micro bicinchoninic acid assay (Pierce Thermo Scientific, 23225), as mentioned above. 4x non-reducing sample dye (250 mM Tris-HCl, pH 6.8; 40% (v:v) glycerol; 8% (w:v) SDS; and 0.01% (w:v) bromophenol blue) was added to the samples. Gelatin zymography was carried out using 10% SDS-polyacrylamide gels with 0.2% (w:v) gelatin. Following electrophoresis, the gels were removed and placed in 2.5% (v:v) Triton X-100 to renature enzymes for 40 min. Then, gels were incubated in 1 M Tris-HCl, 50 mM DTT, pH 7.8 overnight to allow the gelatinolytic activity to occur. Following overnight incubation at 37°C, the gels were incubated with Coomassie stain (0.05% [w:v] Coomassie Brilliant Blue G-250 [Biorad, 1610406], 25% [v:v] methanol, 10% [v/v] acetic acid) for 1 h, followed by destaining (4% [v:v] methanol, 8% [v:v] acetic acid) until clear bands were visible. Gelatinase activity was quantified using ImageJ software.

Enzyme assay.

The cruzipain activity was measured spectrophotometrically at 410 nm with the chromogenic N-Benzoil-Pro-Phe-Arg-p-nitroanilide (0.15 mM, Sigma, B2133) and 520 nm with N-Benzoyl-DL-arginine β-naphthylamides (0.2 mM, Sigma, B4750), at 37°C as previously described [7]. We converted the results into pmol of substrate hydrolyzed per min per mg of protein by using the extinction coefficients 8800 M^{-1} cm^{-1} (p-nitroanilides) and 28000 M^{-1} cm^{-1} (β-naphthylamides), respectively. The activity with the fluorogenic substrate CBZ-Phe-Arg-MCA was assayed at 37°C in a spectrofluorometer (excitation at 370 nm, emission at 460 nm).

Statistical analysis.

Data were expressed as mean ± SE of two or three independent experiments, as detailed in each figure legend. Statistical significance was assessed using Student's t-test or one-way ANOVA test as appropriate (PRISM V. 3.03; GraphPad software). Differences with $p< 0.05$ were considered significant.

Acknowledgments

We want to thank Dr. Wanderley de Souza and Dr. Emile Santos Barrias, who generously gifted the microspheres and shared with us their knowledge about *T. cruzi* compartments. We are also grateful to Rodrigo Militello and Alejandra Medero for their technical assistance.

Disclosure statement

We have not any potential conflict of interest.

References

[1] Moloo A. WHO | World Health Organization. Neglected tropical diseases. 2018.

[2] Sales Junior PA, Molina I, Fonseca Murta SM, et al. Experimental and Clinical Treatment of Chagas Disease: A Review. The American Journal of Tropical Medicine and Hygiene. 2017;97:1289–1303.

[3] Branquinha MH, Oliveira SSC, Sangenito LS, et al. Cruzipain: An Update on its Potential as Chemotherapy Target against the Human Pathogen Trypanosoma cruzi. Current medicinal chemistry. 2015;22:2225–2235.

[4] Jose Cazzulo J, Stoka V, Turk V. The major cysteine proteinase of Trypanosoma cruzi: a valid target for chemotherapy of Chagas disease. Current pharmaceutical design. 2001;7:1143–1156.

[5] Cazzulo JJ. Cruzipain, major cysteine proteinase of Trypanosoma cruzi: sequence and genomic organization of the codifying genes. Medicina. 1999;59 Suppl 2:7–10.

[6] Martínez J, Henriksson J, Ridåker M, et al. Polymorphisms of the genes encoding cruzipain, the major cysteine proteinase of Trypanosoma cruzi, in the region encoding the C-terminal domain. FEMS microbiology letters. 1998;159:35–39.

[7] Alvarez V, Parussini F, Åslund L, et al. Expression in insect cells of active mature cruzipain from trypanosoma cruzi, containing its c-terminal domain. Protein Expression and Purification. 2002;26:467–475.

[8] Sant'Anna C, de Souza W, Cunha-e-Silva N. Biogenesis of the Reservosomes of Trypanosoma cruzi. Microscopy and Microanalysis. 2004;10:637–646.

[9] Cunha-e-Silva NL, Atella GC, Porto-Carreiro IA, et al. Isolation and characterization of a reservosome fraction from *Trypanosoma cruzi*. FEMS Microbiology Letters. 2002;214:7–12.

[10] Huete-Pérez JA, Engel JC, Brinen LS, et al. Protease trafficking in two primitive eukaryotes is mediated by a prodomain protein motif. The Journal of biological chemistry. 1999;274:16249–16256.

[11] Engel JC, Doyle PS, Palmer J, et al. Cysteine protease inhibitors alter Golgi complex ultrastructure and function in Trypanosoma cruzi. Journal of cell science. 1998;111 (Pt 5:597–606).

[12] Reis FCG, Costa TFR, Sulea T, et al. The propeptide of cruzipain − a potent selective inhibitor of the trypanosomal enzymes cruzipain and brucipain, and of the human enzyme cathepsin F. FEBS Journal. 2007;274:1224–1234.

[13] Alvarez VE, Kosec G, Sant'Anna C, et al. Blocking autophagy to prevent parasite differentiation: A possible new strategy for fighting parasitic infections? Autophagy. 2008;4:361–363.

[14] Alvarez VE, Kosec G, Sant'Anna C, et al. Autophagy is involved in nutritional stress response and differentiation in Trypanosoma cruzi. The Journal of biological chemistry. 2008;283:3454–3464.

[15] Klionsky DJ, Abdelmohsen K, Abe A, Abedin MJ, Abeliovich H, Acevedo Arozena A, Adachi H, Adams CM, Adams PD, Adeli K, et al. Guidelines for the use and interpretation of assays for monitoring autophagy (3rd edition). Autophagy 2016; 12:449–50.

[16] Vanrell MC, Losinno AD, Cueto JA, et al. The regulation of autophagy differentially affects Trypanosoma cruzi metacyclogenesis. Buscaglia CA, editor. PLOS Neglected Tropical Diseases. 2017;11:e0006049.

[17] Li FJ, He CY. Acidocalcisome is required for autophagy in Trypanosoma brucei. Autophagy. 2014;10:1978–1988.

[18] Haanstra JR, González-Marcano EB, Gualdrón-López M, et al. Biogenesis, maintenance and dynamics of glycosomes in trypanosomatid parasites. Biochimica et Biophysica Acta (BBA) - Molecular Cell Research. 2016;1863:1038–1048.

[19] Aparicio IM, Scharfstein J, Lima APCA. A new cruzipain-mediated pathway of human cell invasion by Trypanosoma cruzi requires trypomastigote membranes. Infection and immunity. 2004;72:5892–5902.

[20] Ferrão PM, d'Avila-Levy CM, Araujo-Jorge TC, et al. Cruzipain Activates Latent TGF-β from Host Cells during T. cruzi Invasion. Tanowitz HB, editor. PLOS ONE. 2015;10:e0124832.

[21] Tomas AM, Miles MA, Kelly JM. Overexpression of cruzipain, the major cysteine proteinase of Trypanosoma cruzi, is associated with enhanced metacyclogenesis. European journal of biochemistry / FEBS. 1997;244:596–603.

[22] Santos CC, Sant'anna C, Terres A, et al. Chagasin, the endogenous cysteine-protease inhibitor of Trypanosoma

cruzi, modulates parasite differentiation and invasion of mammalian cells. Journal of Cell Science. 2005;118:901–915.

[23] Contreras VT, Araujo-Jorge TC, Bonaldo MC, et al. Biological aspects of the Dm 28c clone of Trypanosoma cruzi after metacyclogenesis in chemically defined media. Memórias do Instituto Oswaldo Cruz. 1999;83:123–133.

[24] Labriola C, Cazzulo JJ, Parodi AJ. Trypanosoma cruz calreticulin is a lectin that binds Monoglucosylated Oligosaccharides but not protein moieties of lycoproteins. Helenius A, editor. Molecular Biology of the Cell. 1999;10:1381–1394.

[25] Campetella O, Martínez J, Cazzulo JJ. A major cysteine proteinase is developmentally regulated in Trypanosoma cruzi. FEMS microbiology letters. 1990;55:145–149.

[26] Engel JC, Torres C, Hsieh I, et al. Upregulation of the secretory pathway in cysteine protease inhibitor-resistant Trypanosoma cruzi. Journal of cell science. 2000;113 (Pt 8):1345–1354.

[27] Soares MJ, Souto-Padrón T, De Souza W. Identification of a large pre-lysosomal compartment in the pathogenic protozoon Trypanosoma cruzi. Journal of cell science. 1992;102 (Pt 1):157–167.

[28] Moreira CMDN, Batista CM, Fernandes JC, et al. Knockout of the gamma subunit of the AP-1 adaptor complex in the human parasite Trypanosoma cruzi impairs infectivity and differentiation and prevents the maturation and targeting of the major protease cruzipain. PLoS ONE. 2017;12:1–22.

[29] Barisón MJ, Rapado LN, Merino EF, et al. Metabolomic profiling reveals a finely tuned, starvation-induced metabolic switch in Trypanosoma cruzi epimastigotes. The Journal of biological chemistry. 2017;292:8964–8977.

[30] McKerrow JH, Rosenthal PJ, Swenerton R, et al. Development of protease inhibitors for protozoan infections. Current Opinion in Infectious Diseases. 2008;21:668–672.

[31] Liu J, Xia H, Kim M, et al. Beclin1 controls the levels of p53 by regulating the deubiquitination activity of USP10 and USP13. Cell. 2011;147:223–234.

[32] Barclay JJ, Morosi LG, Vanrell MC, et al. Trypanosoma cruzi Coexpressing Ornithine Decarboxylase and Green Fluorescence Proteins as a Tool to Study the Role of Polyamines in Chagas Disease Pathology. Enzyme research. 2011;2011:657460.

[33] de Souza W, de Carvalho TMU, Barrias ES. Review on Trypanosoma cruzi: Host Cell Interaction. International journal of cell biology. 2010;2010:1–18.

[34] Vidal JC, Alcantara C de L, de Souza W, et al. Loss of the cytostome-cytopharynx and endocytic ability are late events in Trypanosoma cruzi metacyclogenesis. Journal of structural biology. 2016;196:319–328.

[35] Trocoli Torrecilhas AC, Tonelli RR, Pavanelli WR, et al. Trypanosoma cruzi: parasite shed vesicles increase heart parasitism and generate an intense inflammatory response. Microbes and infection. 2009;11:29–39.

[36] Bayer-Santos E, Cunha-e-Silva NL, Yoshida N, et al. Expression and cellular trafficking of GP82 and GP90 glycoproteins during Trypanosoma cruzi metacyclogenesis. Parasites & Vectors. 2013;6:127. A

[37] Garcia-Silva MR, Cura das Neves RF, Cabrera-Cabrera F, et al. Extracellular vesicles shed by Trypanosoma cruzi are linked to small RNA pathways, life cycle regulation, and susceptibility to infection of mammalian cells. Parasitology Research. 2014;113:285–304.

[38] Docampo R, Ulrich P, Moreno SNJ. Evolution of acidocalcisomes and their role in polyphosphate storage and osmoregulation in eukaryotic microbes. Philosophical Transactions of the Royal Society B: Biological Sciences. 2010;365:775–784.

[39] Hellman U, Wernstedt C, Cazzulo JJ. Self-proteolysis of the cysteine proteinase, cruzipain, from Trypanosoma cruzi gives a major fragment corresponding to its carboxy-terminal domain. Molecular and biochemical parasitology. 1991;44:15–21.

[40] McKerrow JH, Doyle PS, Engel JC, et al. Two approaches to discovering and developing new drugs for Chagas disease. Memorias do Instituto Oswaldo Cruz. 2009;104 Suppl 1:263–269.

[41] Scharfstein J, Schmitz V, Morandi V, et al. Host Cell Invasion by *Trypanosoma Cruzi* Is Potentiated by Activation of Bradykinin B_2 Receptors. The Journal of Experimental Medicine. 2000;192:1289–1300.

[42] Cazzulo JJ. Intermediate metabolism in Trypanosoma cruzi. Journal of bioenergetics and biomembranes. 1994;26:157–165.

[43] San Francisco J, Barría I, Gutiérrez B, et al. Decreased cruzipain and gp85/trans-sialidase family protein expression contributes to loss of Trypanosoma cruzi trypomastigote virulence. Microbes and infection. 2017;19:55–61.

[44] Stoka V, Nycander M, Lenarcic B, et al. Inhibition of cruzipain, the major cysteine proteinase of the protozoan parasite, Trypanosoma cruzi, by proteinase inhibitors of the cystatin superfamily. FEBS letters. 1995;370:101–104.

[45] Fader CM, Aguilera MO, Colombo MI. ATP is released from autophagic vesicles to the extracellular space in a VAMP7-dependent manner. Autophagy. 2012;8:1741–1756.

[46] Ramirez MI, Yamauchi LM, de Freitas LH, et al. The use of the green fluorescent protein to monitor and improve transfection in Trypanosoma cruzi. Molecular and biochemical parasitology. 2000;111:235–240.

[47] Ferreira LRP, Dossin F de M, Ramos TC, et al. Active transcription and ultrastructural changes during Trypanosoma cruzi metacyclogenesis. Anais da Academia Brasileira de Ciencias. 2008;80:157–166.

[48] Bolte S, Cordelières FP. A guided tour into subcellular colocalization analysis in light microscopy. Journal of microscopy. 2006;224:213–232.

[49] Linda J. Herrera; Stephen Brand; Andres Santos; Lilian L. Nohara; Justin Harrison; Neil R. Norcross; Stephen Thompson; Victoria Smith; Carolina Lema; Armando Varela-Ramirez; Ian H. Gilbert; Igor C. Almeida; Rosa A. Maldonado. Validation of N -myristoyltransferase as Potential Chemotherapeutic Target in Mammal-Dwelling Stages of Trypanosoma cruzi. 2016;1–20.

Figure Legends

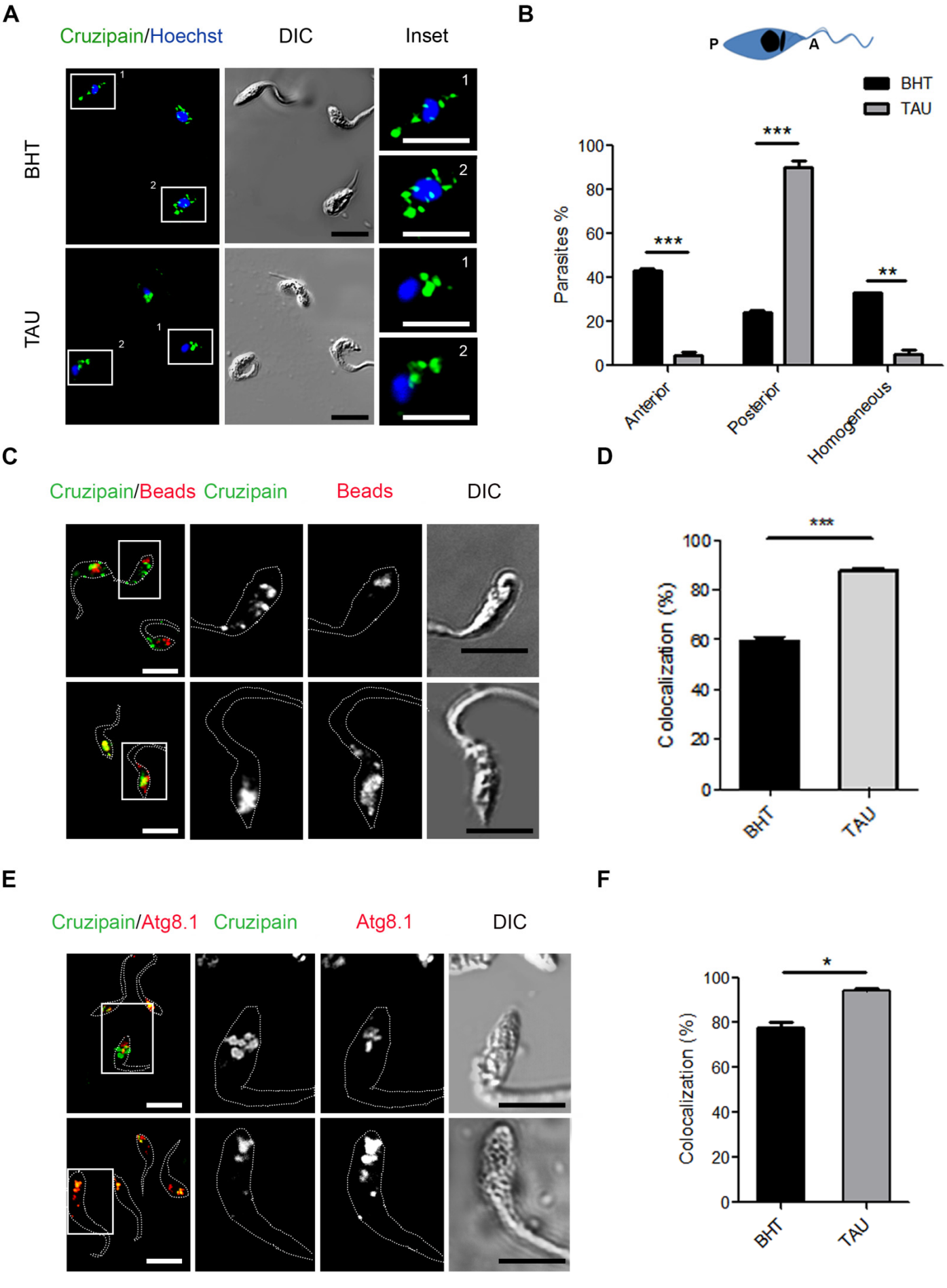
A
Cruzipain/Hoechst
DIC
Inset
BHT
TAU
B
P
A
BHT
TAU
Parasites %
100
80
60
40
20
0
***
***
**
Anterior
Posterior
Homogeneous
C
Cruzipain/Beads
Cruzipain
Beads
DIC
D
***
Colocalization (%)
100
80
60
40
20
0
BHT
TAU
E
Cruzipain/Atg8.1
Cruzipain
Atg8.1
DIC
F
*
Colocalization (%)
100
80
60
40
20
0
BHT
TAU

Figure 1. Induction of autophagy accumulates cruzipain in reservosomes. (**A**) Immunofluorescence analysis of cruzipain distribution in epimastigotes (Y WT strain) exposed to the first stage of metacyclogenesis under optimal nutritional conditions (BHT) or nutritional stress as an autophagy stimulus (TAU). Parasites' boundaries are depicted by white dashed lines. Scale bars: 5 μm. (**B**) Quantification of parasites that present some of the cruzipain distribution patterns (Anterior, Posterior or Homogeneous) according to the nutritional condition. Data are shown as mean ± error of three independent experiments. A total of 100 parasites per group for each experiment were quantified. P values were calculated using the Student 2-tailed unpaired t-test. (**) $p \leq 0.01$, (***) $p \leq 0.001$. (**C**) Immunofluorescence analysis of cruzipain distribution respect to fluorescent beads (late endosome marker) in epimastigotes (Y WT strain) at the end of the first stage of metacyclogenesis with BHT or TAU treatment. Parasites' boundaries are depicted by white dashed lines. Scale bars: 5 μm. (**D**) Quantification of colocalization degree of cruzipain with fluorescent beads according to the nutritional condition. Data are shown as mean ± error of three independent experiments. A total of 50 parasites per group for each experiment were quantified. P values were calculated using the Student 1-tailed unpaired t-test. (***) $p \leq 0.001$. (**E**) Immunofluorescence analysis of cruzipain disposition respect to the Tc Atg8.1 protein (autophagic marker) in epimastigotes (Y WT strain) induced to undergo autophagy (TAU) or not (BHT) during the first stage of metacyclogenesis. Parasites' boundaries are depicted by white dashed lines. Scale bars: 5 μm. (**F**) Quantification of colocalization degree of cruzipain with Tc Atg8.1 protein according to the nutritional condition. Data are shown as mean ± error of three independent experiments. A total of 50 parasites per group for each experiment were quantified. P values were calculated using Student's 2-tailed unpaired t-test. (*) $p \leq 0.05$.

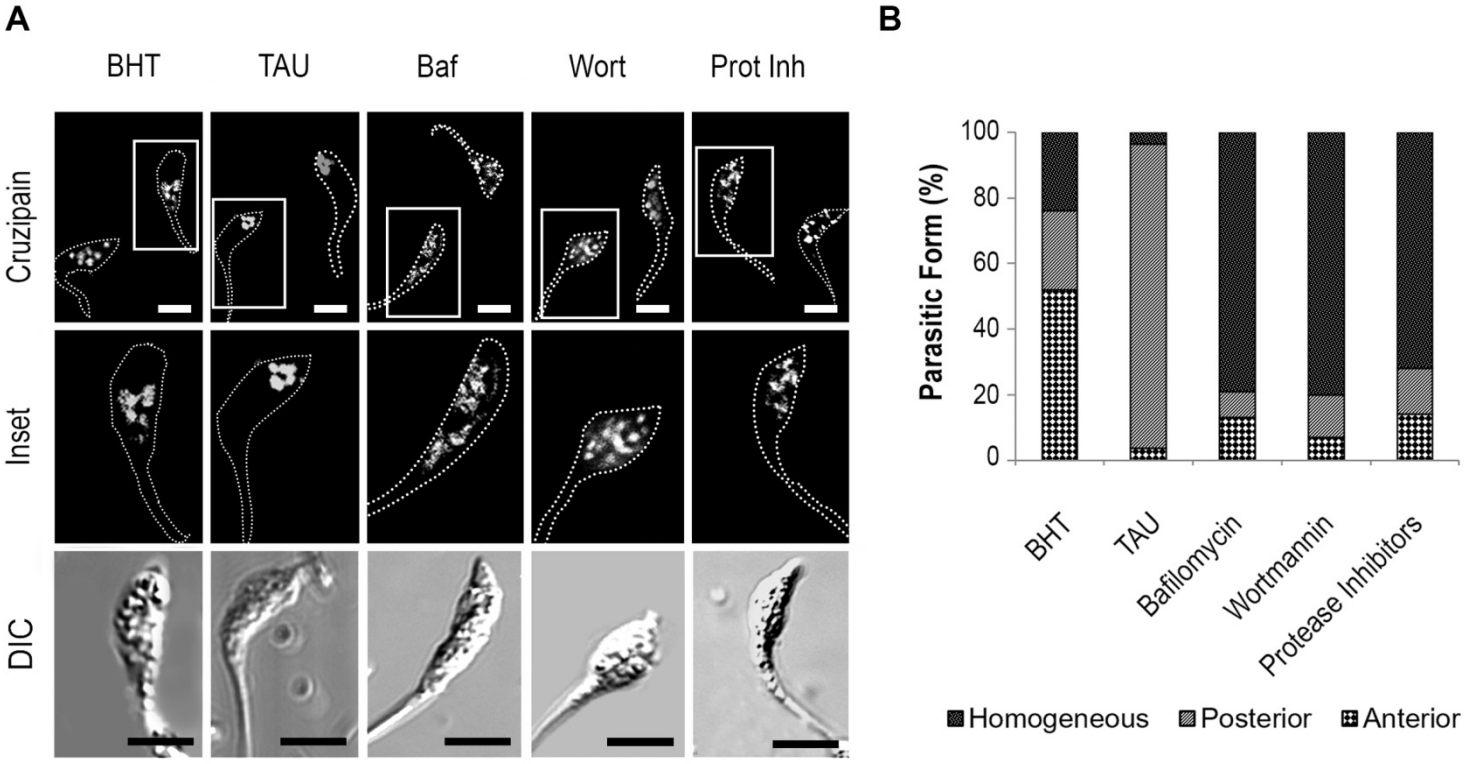
A
BHT
TAU
Baf
Wort
Prot Inh
Cruzipain
Inset
DIC
B
Parasitic Form (%)
100
80
60
40
20
0
BHT
TAU
Bafilomycin
Wortmannin
Protease Inhibitors
Homogeneous
Posterior
Anterior

Figure 2. Inhibition of autophagy and hydrolytic activity maintain cruzipain in the homogeneous distribution. (**A**) Immunofluorescence analysis of cruzipain distribution in epimastigotes (Y WT strain) exposed to the first stage of metacyclogenesis under BHT and TAU treatment with or without the addition of autophagy inhibitors (Baf or Wort) or broad-spectrum protease inhibitors (Prot Inh). Parasites' boundaries are depicted by white dashed lines. Scale bars: 5 μm. (**B**) Quantification of the relative number of parasites that present some of the cruzipain distribution patterns (Anterior, Posterior, or Homogeneous) according to the treatment with inhibitors at the end of the first stage of metacyclogenesis. Data are shown as the mean of three independent experiments. A total of 50 parasites per group for each experiment were quantified.

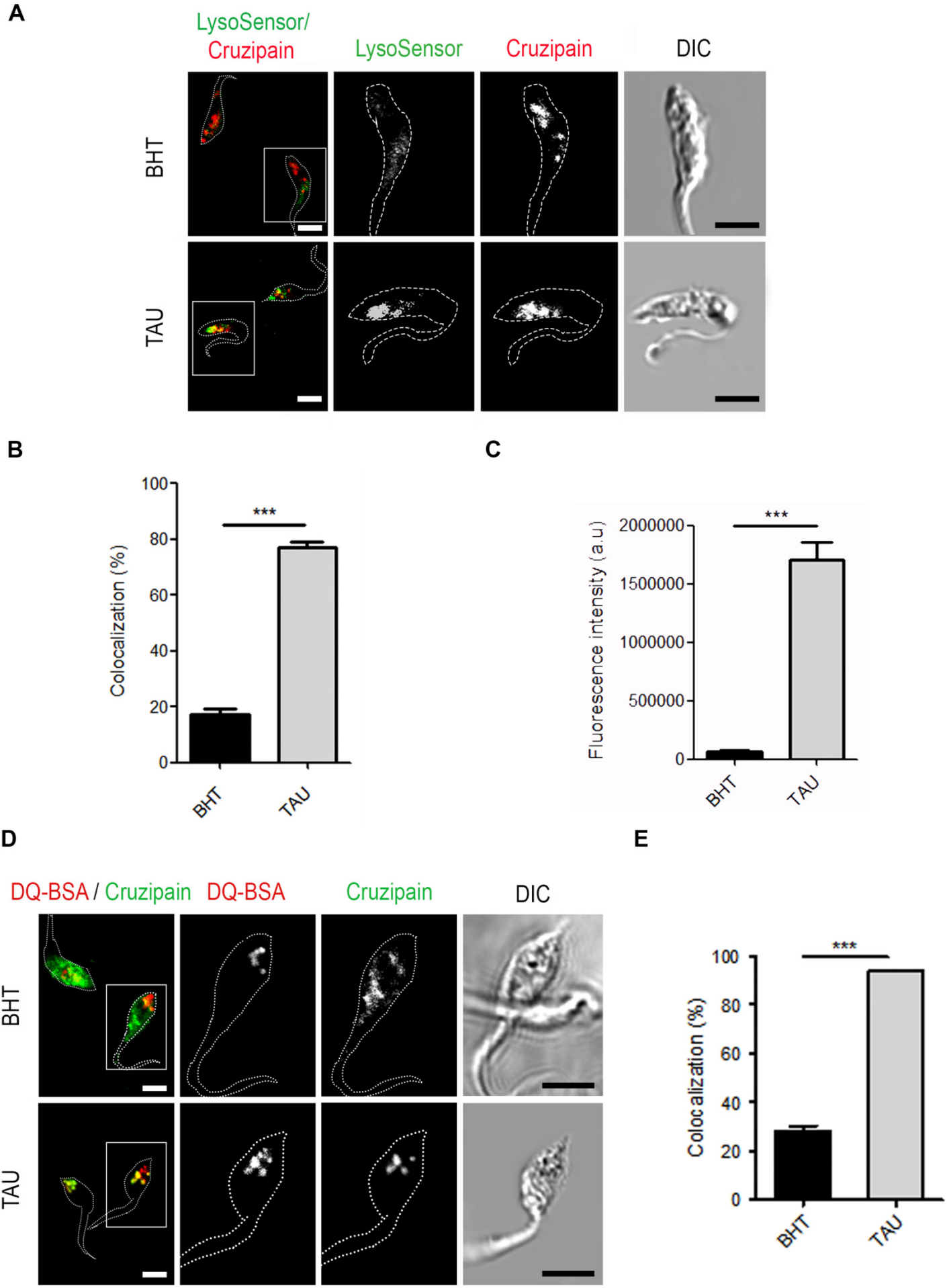
A
LysoSensor/
Cruzipain
LysoSensor
Cruzipain
DIC
BHT
TAU
B
Colocalization (%)
100
80
60
40
20
0
***
BHT
TAU
C
Fluorescence intensity (a.u)
2000000
1500000
1000000
500000
0
***
BHT
TAU
D
DQ-BSA / Cruzipain
DQ-BSA
Cruzipain
DIC
BHT
TAU
E
Colocalization (%)
100
80
60
40
20
0
***
BHT
TAU

Figure 3. Induction of autophagy transforms reservosomes in hydrolytic compartments. (**A**) Variability of cruzipain-positive compartments acidity in epimastigotes (Y WT strain) exposed to the first stage of metacyclogenesis under optimal nutritional conditions or nutritional stress and stained with LysoSensor dye. Fluorescence images corresponding to this pH-sensitive dye were acquired using 1,000 ms exposure. Parasites' boundaries are depicted by white dashed lines. Scale bars: 5 μm. (**B**) Quantification of colocalization degree of cruzipain with the acidic compartments stained with LysoSensor in relation to BHT/TAU treatment. Data are shown as mean ± error of two independent experiments. A total of 50 parasites per group for each experiment were quantified. P values were calculated using the Student 1-tailed unpaired t-test. (***) p≤0.001. (**C**) Quantification of fluorescence intensity of LysoSensor according to the nutritional condition. Data are shown as mean ± error of two independent experiments. A total of 50 parasites per group for each experiment were quantified. P values were calculated using Student's 2-tailed unpaired t-test. (***) p≤0.001. (**D**) Immunofluorescence analysis of cruzipain distribution in relation to the hydrolytic marker DQ-BSA in epimastigotes (Y WT strain) induced to undergo autophagy (TAU) or not (BHT) during the first stage of metacyclogenesis. Parasites' boundaries are depicted by white dashed lines. Scale bars: 5 μm. (**E**) Quantification of the colocalization degree between cruzipain-positive compartments with those compartments that have hydrolytic activity. Data are shown as mean ± error of three independent experiments. A total of 50 parasites per group for each experiment were quantified. P values were calculated using the Student 2-tailed unpaired t-test. (***) p≤0.001.

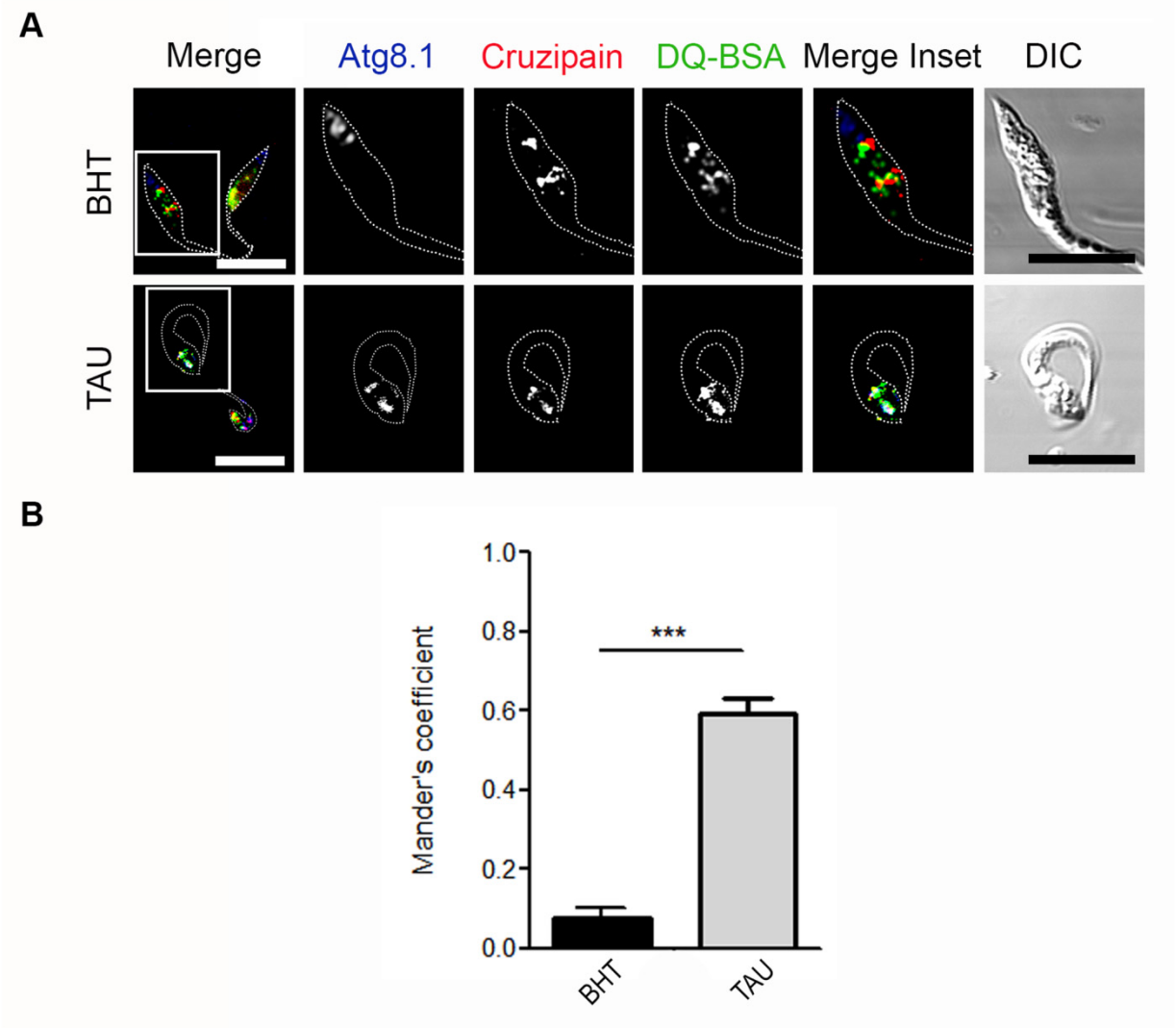
A
Merge
Atg8.1
Cruzipain
DQ-BSA
Merge Inset
DIC
BHT
TAU
B
Mander's coefficient
1.0
0.8
0.6
0.4
0.2
0.0
***
BHT
TAU

Figure 4. Autophagy induces the increase of colocalization between cruzipain, Atg8.1, and DQ-BSA-positive compartments. (**A**) Immunofluorescence analysis of triple colocalization between cruzipain, Atg8.1 and the hydrolytic marker DQ-BSA in epimastigotes (Y WT strain) exposed to the complete differentiation cycle (72 h) under optimal nutritional conditions (BHT) or nutritional stress (TAU). Parasites' boundaries are depicted by white dashed lines. Scale bars: 5 μm. (**B**) Quantification of Mander's coefficients corresponding to the triple colocalization between cruzipain-positive compartments with those autophagic and hydrolytic compartments. Data are shown as mean ± error of two independent experiments. A total of 20 parasites per group for each experiment were quantified. P values were calculated using the Student 2-tailed unpaired t-test. (***) $p \leq 0.001$.

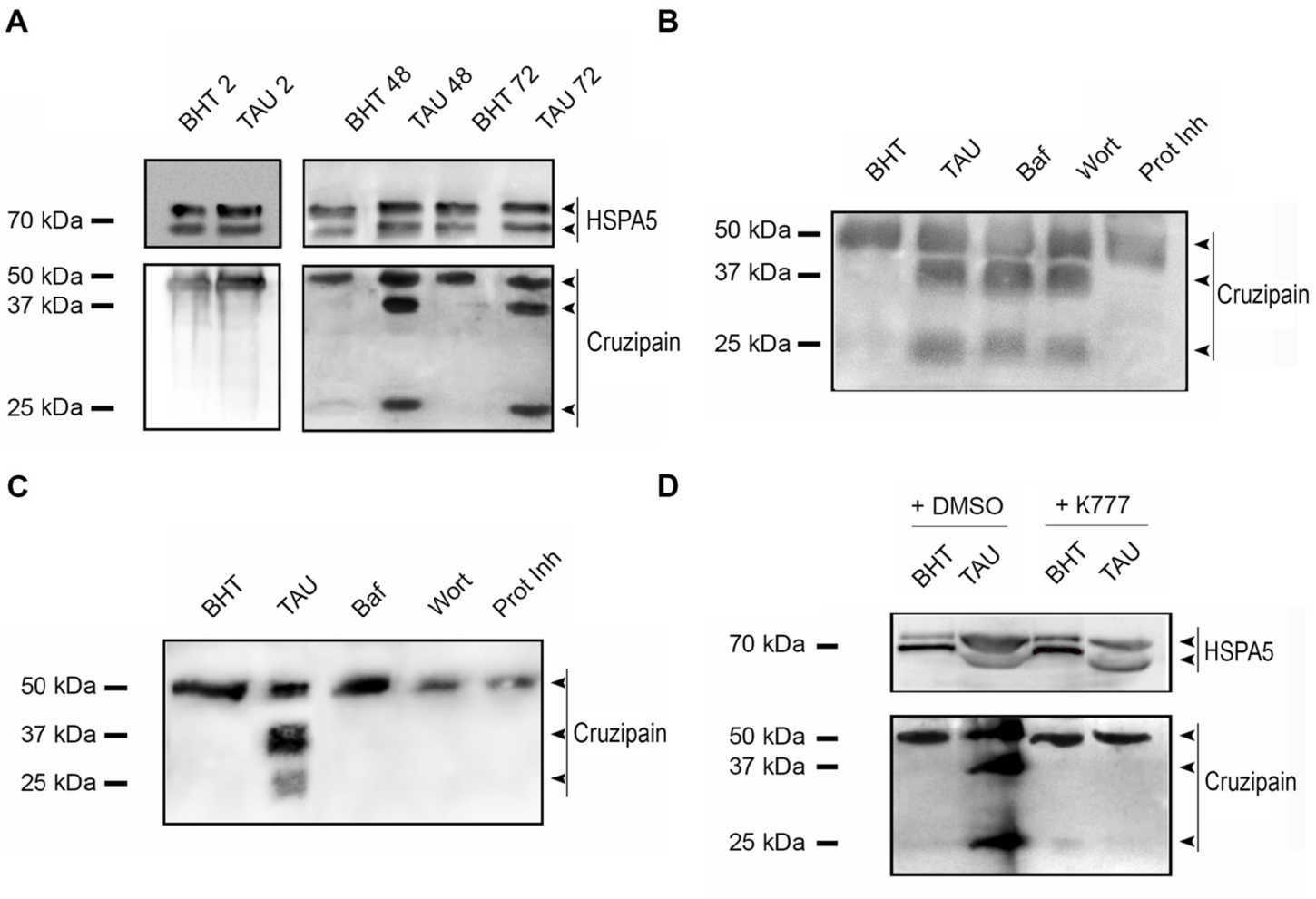
A
BHT 2
TAU 2
BHT 48
TAU 48
BHT 72
TAU 72
70 kDa
50 kDa
37 kDa
25 kDa
HSPA5
Cruzipain
B
BHT
TAU
Baf
Wort
Prot Inh
50 kDa
37 kDa
25 kDa
Cruzipain
C
BHT
TAU
Baf
Wort
Prot Inh
50 kDa
37 kDa
25 kDa
Cruzipain
D
+ DMSO
+ K777
BHT
TAU
BHT
TAU
70 kDa
50 kDa
37 kDa
25 kDa
HSPA5
Cruzipain

Figure 5. Inhibition of autophagy prevents cruzipain processing during *T. cruzi* metacyclogenesis. (**A**) Western blot analysis of cruzipain in total protein extracts from epimastigotes exposed to *in vitro* metacyclogenesis. Samples were collected after 2 h (first stage), 48 h or 72 h (complete differentiation cycle) and lysates were obtained. The different forms of cruzipain (mature form with 50 kDa, partially degraded form with 37 kDa and the C-terminal extension with 25 kDa) that results from its autocatalytic activity were detected with a polyclonal antibody against this protein. The arrowheads indicate the position of each cruzipain form in the order established above. A double band of HSPA5 was also detected with a specific antibody and used as a loading control. Images are representative of three independent experiments (**B and C**) Western blot analysis of cruzipain from total protein extracts of epimastigotes exposed to *in vitro* metacyclogenesis in the presence of autophagy inhibitors (Baf or Wort) or broad-spectrum protease inhibitors (Prot Inh) only in the first stage (**B**) or in the complete cycle (**C**). Samples were collected at 72 h, and lysates were obtained. The different forms of cruzipain were detected with a polyclonal antibody against this protein. The arrowheads indicate the position of each cruzipain form in the order established above. Image is representative of three independent experiments. (**D**) Western blot analysis of cruzipain from total protein extracts of epimastigotes exposed to *in vitro* metacyclogenesis in the absence (DMSO) or presence of K777 drug, a specific cruzipain inhibitor, during the complete cycle. Samples were collected at 72 h and lysates were obtained and processed as above. The arrowheads indicate the position of the mature and processed enzyme in the order established above. Images are representative of three independent experiments.

A

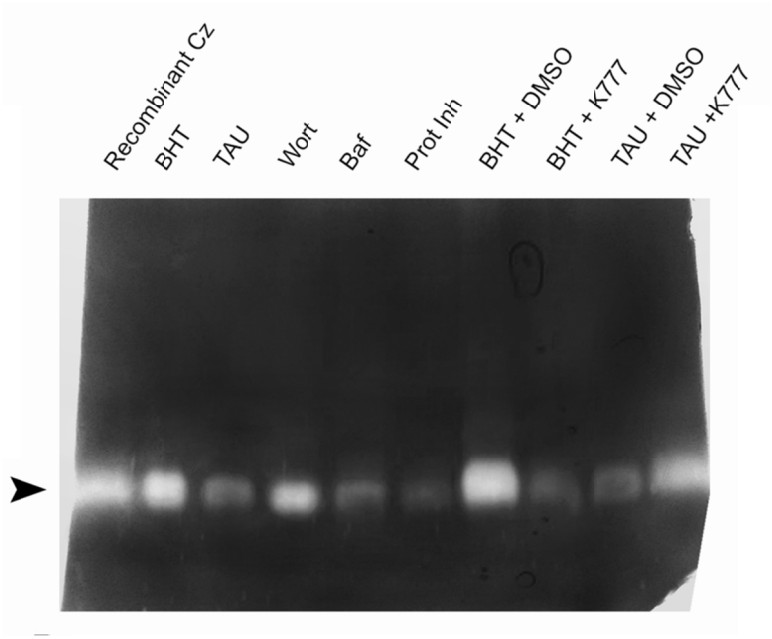
Recombinant Cz
BHT
TAU
Wort
Baf
Prot Inh
BHT + DMSO
BHT + K777
TAU + DMSO
TAU +K777

B

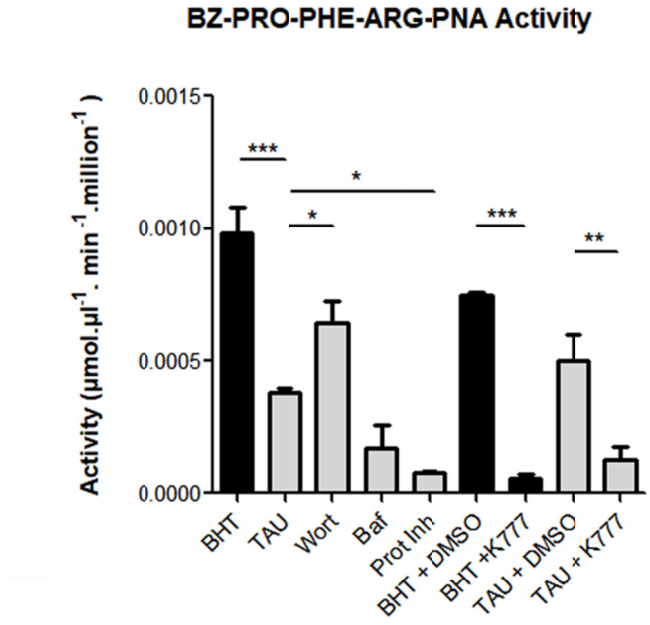
BZ-PRO-PHE-ARG-PNA Activity
Activity (µmol.µl-1. min-1.million-1)
0.0015
0.0010
0.0005
0.0000
***
*
*
***
**
BHT
TAU
Wort
Baf
Prot Inh
BHT + DMSO
BHT +K777
TAU + DMSO
TAU + K777

Figure 6. Inhibition of autophagy decreases cruzipain activity during *T. cruzi* differentiation. (**A**) Enzyme assay of total protein extracts from epimastigotes exposed to *in vitro* metacyclogenesis in the absence or presence of autophagy inhibitors (Baf or Wort), broad-spectrum protease inhibitors (Prot Inh) or K777 drug. Inhibition treatments were made during the complete differentiation cycle, and samples were collected at 72 h to obtain lysates for gel zymography (**A**) or the reaction with the fluorogenic substrate CBZ-Phe-Arg-MCA (**B**). In the last case, enzyme activity was assayed at 37°C in a spectrofluorometer (excitation at 370 nm, emission at 460 nm) and the results were converted into μmol of substrate hydrolyzed per min per mg of protein. Arrowhead indicates the position of mature cruzipain. Image (**A**) and data (**B**) are representative of three independent experiments.

A

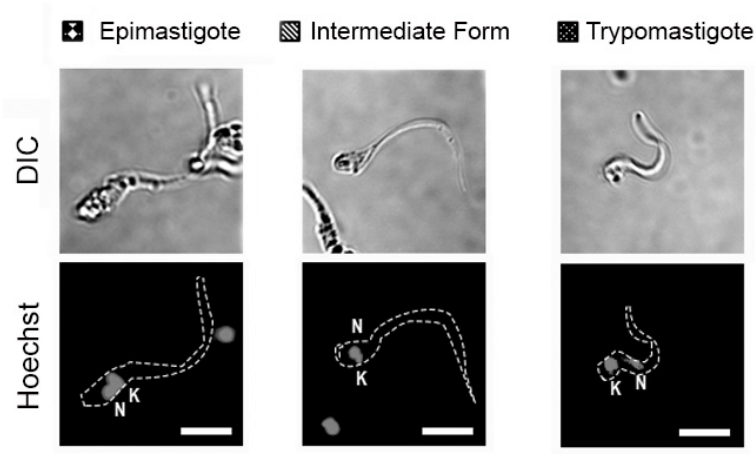
Epimastigote
Intermediate Form
Trypomastigote
DIC
Hoechst
N
K
N
K
K
N

B

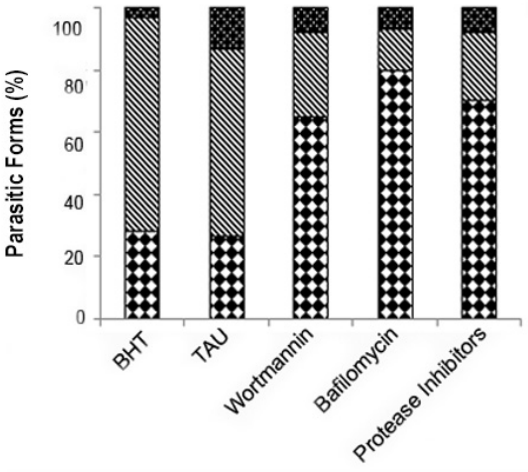
Parasitic Forms (%)
100
80
60
40
20
0
BHT
TAU
Wortmannin
Bafilomycin
Protease Inhibitors

C

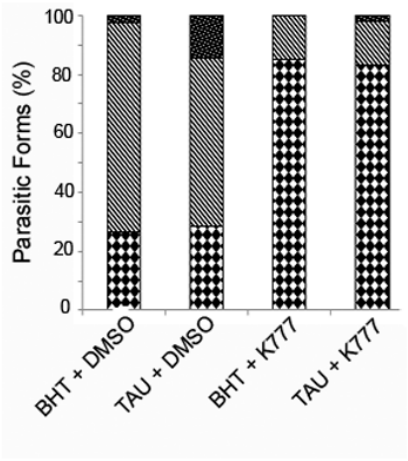
Parasitic Forms (%)
100
80
60
40
20
0
BHT + DMSO
TAU + DMSO
BHT + K777
TAU + K777

Figure 7. Activation of cruzipain is a key process during metacyclogenesis. Quantification of relative number of epimastigotes, intermediate forms and metacyclic forms obtained at 72 h from parasites (Y WT strain) exposed to *in vitro* metacyclogenesis in absence or in presence of autophagy inhibitors (Baf or Wort), broad-spectrum protease inhibitors (Prot Inh) (**A**) or K777 drug (**B**), which were added during the complete differentiation cycle. Data are shown as the mean of three independent experiments. A total of 50 parasites per group for each experiment were quantified.

A

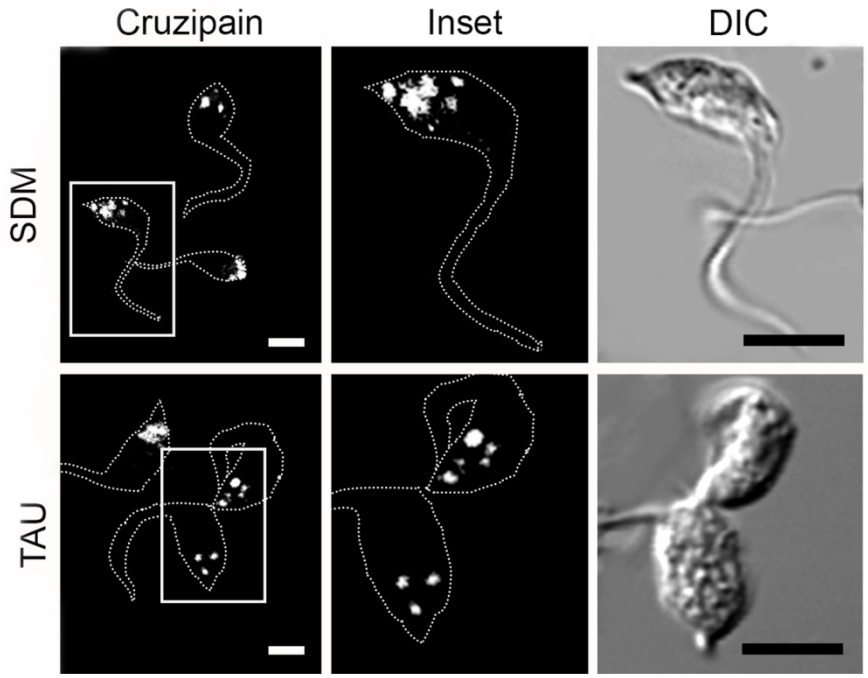
Cruzipain
Inset
DIC
SDM
TAU

B

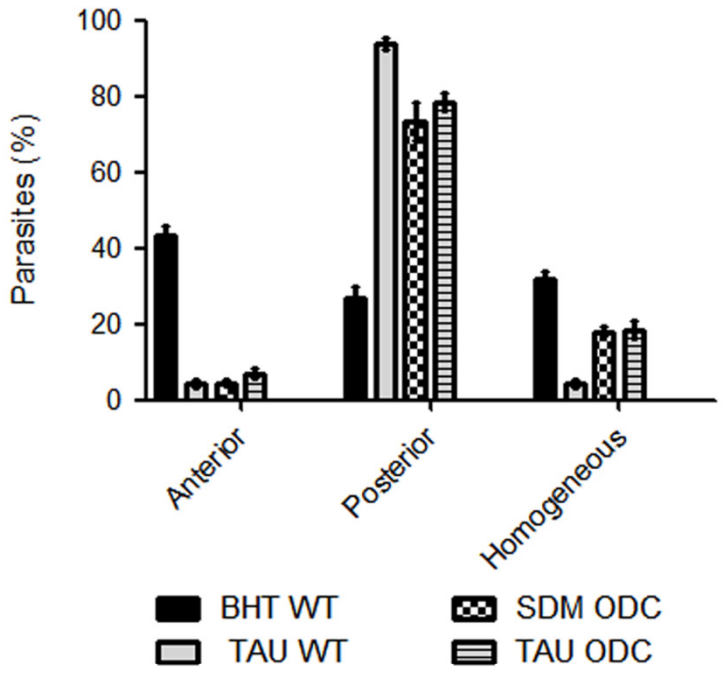
Parasites (%)
100
80
60
40
20
0
Anterior
Posterior
Homogeneous
BHT WT
TAU WT
SDM ODC
TAU ODC

C

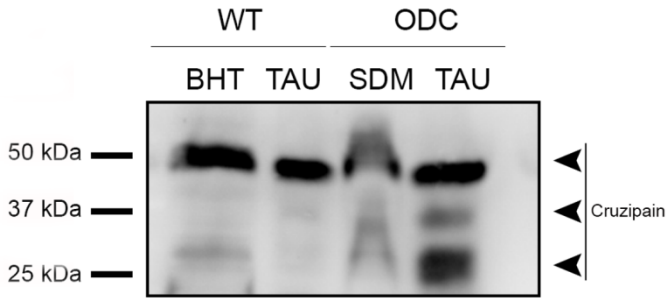
WT
ODC
BHT
TAU
SDM
TAU
50 kDa
37 kDa
25 kDa
Cruzipain

Figure 8. Cruzipain is highly processed in a mutant strain with activated autophagy. (**A**) Immunofluorescence analysis of cruzipain distribution in epimastigotes (Y-GFP-ODC strain) exposed to the first stage of metacyclogenesis under optimal nutritional conditions (SDM) or nutritional stress as an autophagy stimulus (TAU). Parasites' boundaries are depicted by white dashed lines. Scale bars: 5 μm. (**B**) Quantification of parasites that present some of the cruzipain distribution patterns (Anterior, Posterior or Homogeneous) according to the nutritional condition. Data are shown as mean ± error of three independent experiments. A total of 100 parasites per group for each experiment were quantified. P values were calculated using Student's 2-tailed unpaired t-test. (***) p≤0.001. (**C**) Western blot analysis of cruzipain in total protein extracts from epimastigotes (Y-GFP strain vs. Y-GFP-ODC strain) exposed to *in vitro* metacyclogenesis. Samples were collected after 2 h (first stage) and lysates were obtained. The different forms of cruzipain were detected with a polyclonal antibody against this protein. The arrowheads indicate the position of each cruzipain form in the order established above. Image is representative of three independent experiments.

A

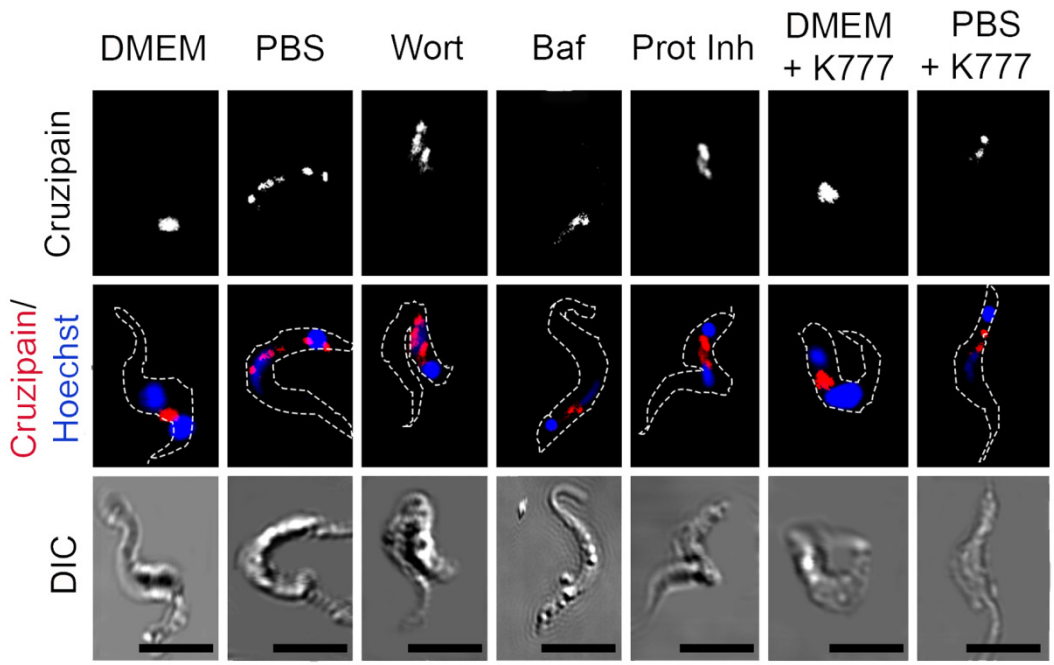
DMEM
PBS
Wort
Baf
Prot Inh
DMEM + K777
PBS + K777
Cruzipain
Cruzipain/ Hoechst
DIC

B

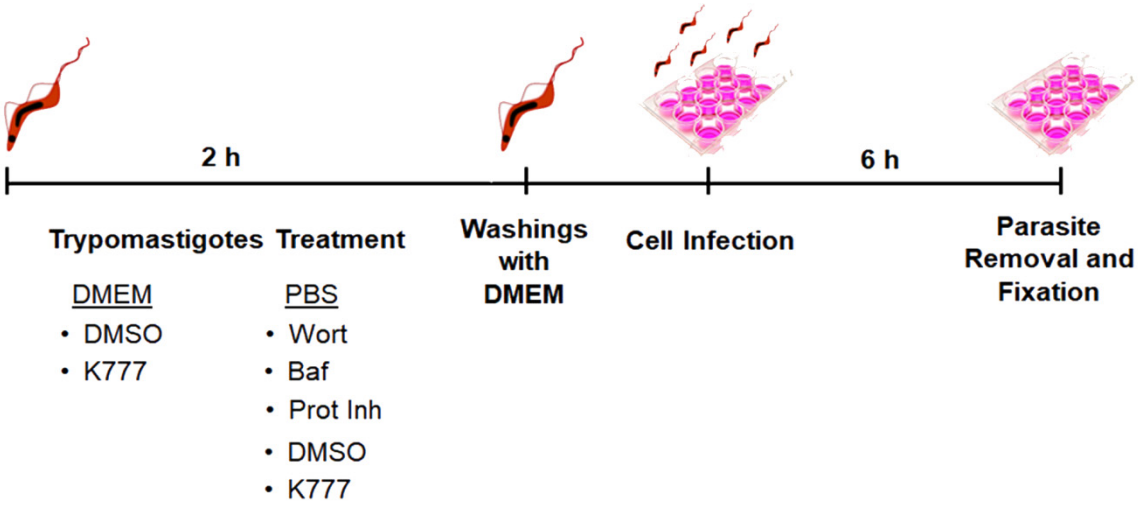
2 h
6 h
Trypomastigotes Treatment
DMEM
• DMSO
• K777
PBS
• Wort
• Baf
• Prot Inh
• DMSO
• K777
Washings with DMEM
Cell Infection
Parasite Removal and Fixation

C

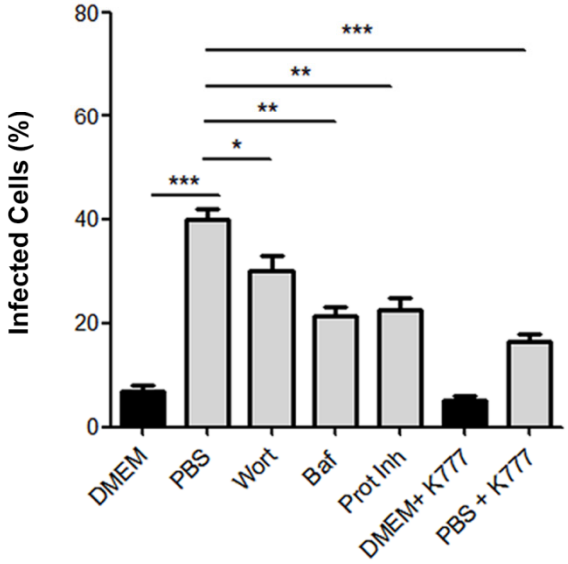
Infected Cells (%)
80
60
40
20
0
***
**
**
*
***
DMEM
PBS
Wort
Baf
Prot Inh
DMEM+ K777
PBS + K777

Figure 9. Cruzipain is required during *T. cruzi* infection into the host cell. (**A**) Immunofluorescence of cruzipain distribution in metacyclic trypomastigotes. Parasites' boundaries are depicted by white dashed lines. Scale bar: 5 µm. (**B**) Representative scheme of the infection protocol. (**C**) Percentage of the infected cell (after 6 h) by trypomastigotes pretreated with the maintenance medium (DMEM or PBS) in the presence or not of autophagy inhibitors (Baf or Wort), broad-spectrum protease inhibitors (Prot Inh) or with K777 drug for 2 h. Data are shown as mean ± error of three independent experiments. A total of 100 cells per group for each experiment were quantified. P values were calculated using the One-way ANOVA test. (*) $p \leq 0.05$, (**) $p \leq 0.01$, (***) $p \leq 0.001$.

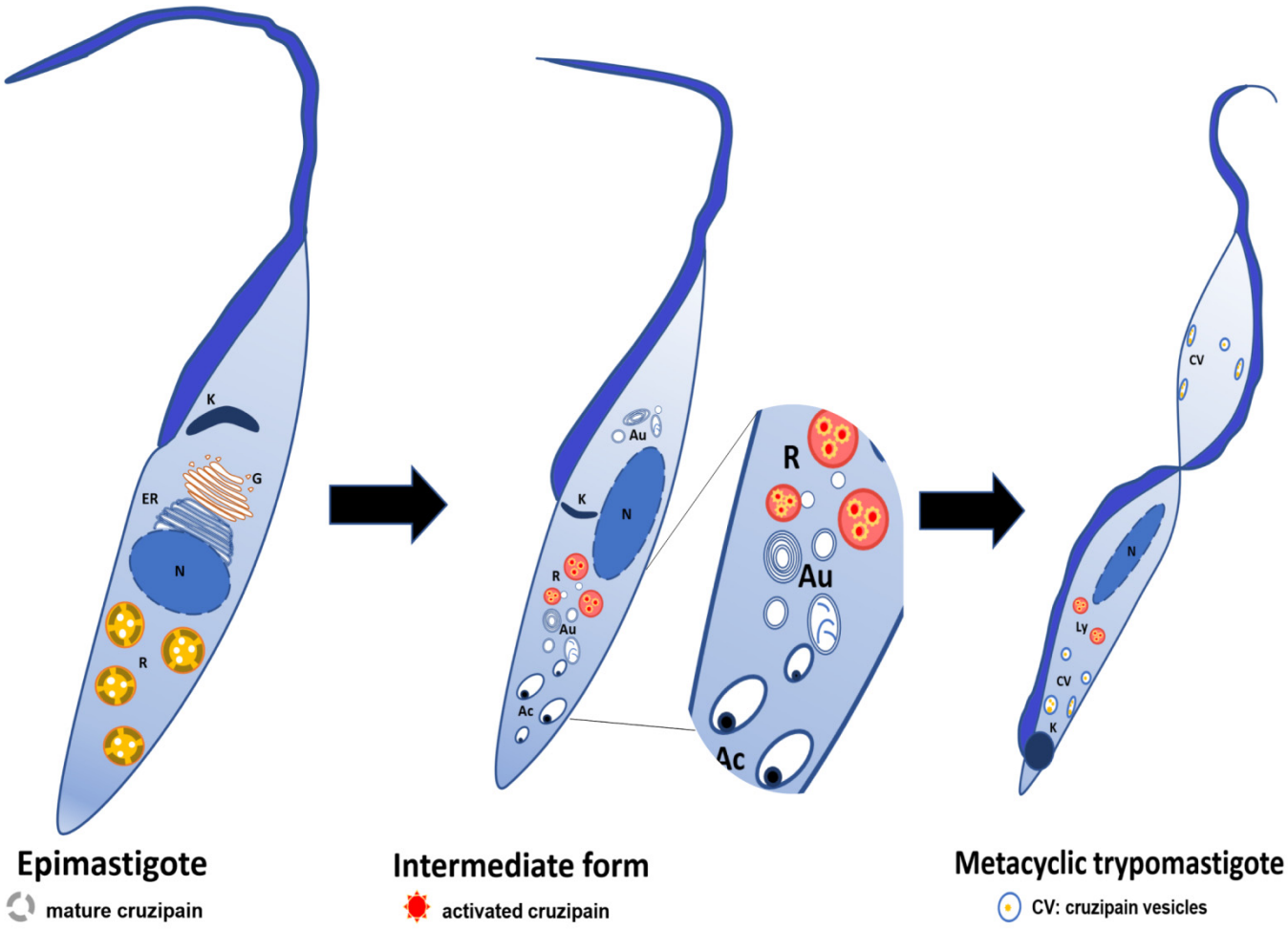
K
G
ER
N
R
Au
K
N
R
Au
Ac
R
Au
Ac
CV
N
Ly
CV
K
Epimastigote
mature cruzipain
Intermediate form
activated cruzipain
Metacyclic trypomastigote
CV: cruzipain vesicles

Figure 10. Proposed model of participation of autophagy during *T. cruzi* metacyclogenesis. In epimastigotes, cruzipain precursors are found in the compartments of the biosynthetic-secretory pathway whereas mature Cz is collected in reservosomes. Autophagy induction during *T. cruzi* metacyclogenesis promotes the fusion of autophagosomes (possibly derived from acidocalcisomes) to reservosomes. As a result of this interaction, reservosomes turned more acidic and hydrolytic, Cz increases its activity and finally undergo self-proteolysis (Intermediate structure). Newly differentiated metacyclic trypomastigotes displayed Cz in lysosomes and also in vesicles located close to the plasma membrane, a position that is enhanced in starved trypomastigotes. K: kinetoplast, G: Golgi apparatus, ER: endoplasmic reticulum, N: nucleus, R: reservosomes, Au: autophagosomes, Ac: acidocalcisomes, Ly: lysosomes, CV; cruzipain vesicles.

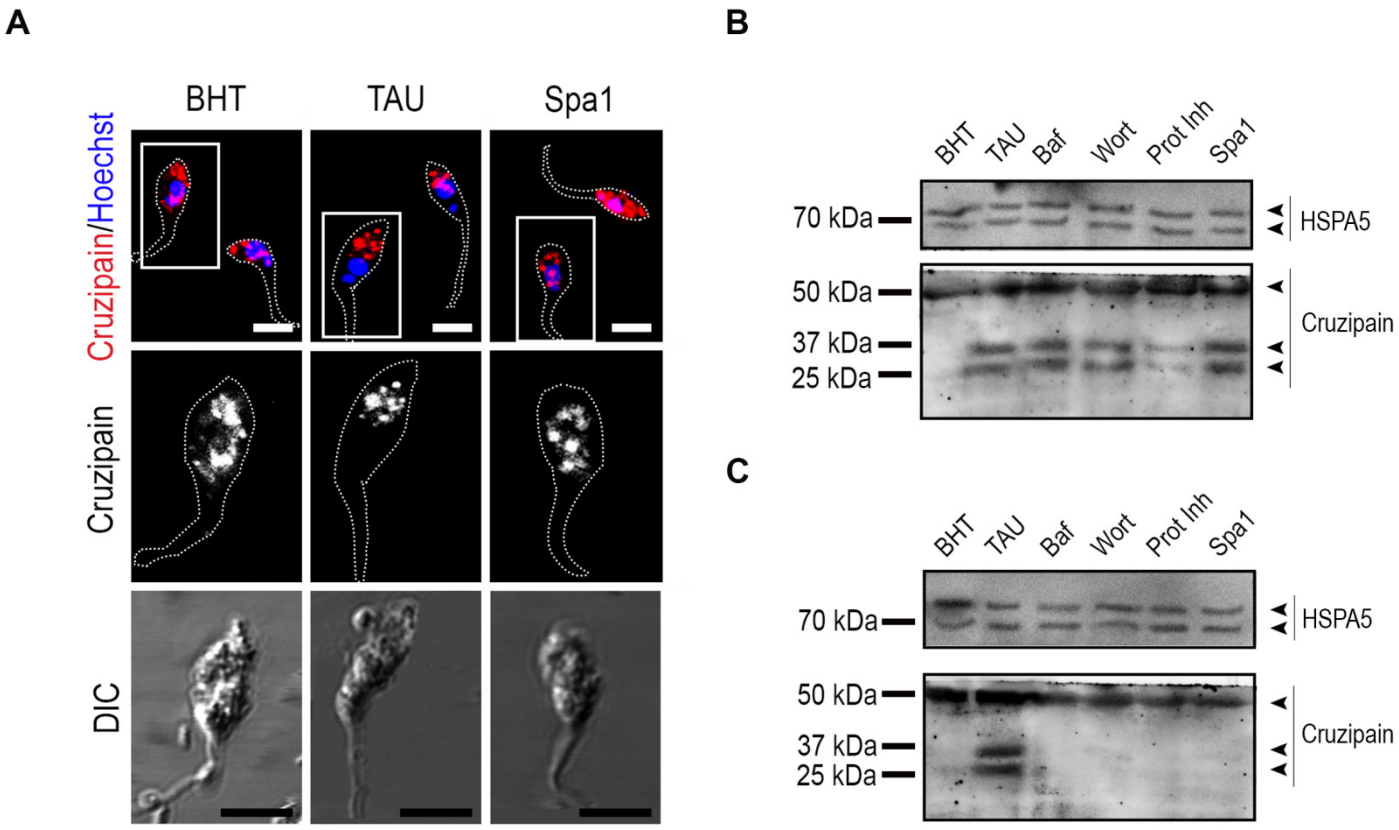
A
BHT
TAU
Spa1
Cruzipain/Hoechst
Cruzipain
DIC
B
BHT
TAU
Baf
Wort
Prot Inh
Spa1
70 kDa
50 kDa
37 kDa
25 kDa
HSPA5
Cruzipain
C
BHT
TAU
Baf
Wort
Prot Inh
Spa1
70 kDa
50 kDa
37 kDa
25 kDa
HSPA5
Cruzipain

Figure S1. Inhibition of autophagy by Spautin-1 impairs normal Cz localization and processing during *T. cruzi* metacyclogenesis. (**A**) Immunofluorescence analysis of cruzipain distribution in epimastigotes (Y WT strain) exposed to the first stage of metacyclogenesis under BHT, TAU and TAU treatment with the addition of Spautin-1 (Spa1). Parasites' boundaries are depicted by white dashed lines. Scale bars: 5 μm. Images are representative of two independent experiments. Western blot analysis of cruzipain from total protein extracts of epimastigotes exposed to *in vitro* metacyclogenesis in presence of autophagy inhibitors (Baf, Wort or Spa1) or broad-spectrum protease inhibitors (Prot Inh) only in the first stage (**B**) or in the complete cycle (**C**). Samples were collected at 72 h and lysates were obtained. The different forms of cruzipain were detected with a polyclonal antibody against this protein. The arrowheads indicate the position of each cruzipain form. Images are representative of two independent experiments.

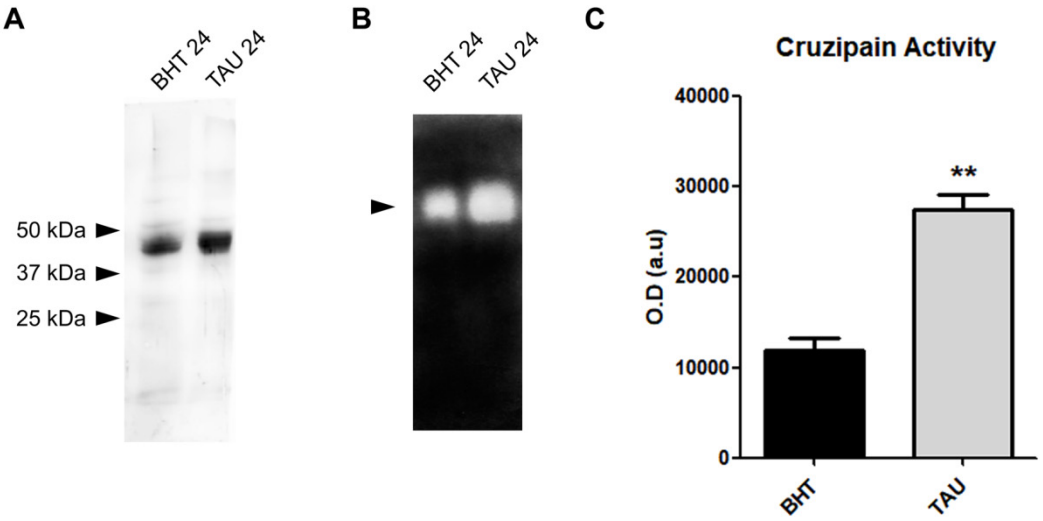
A
BHT 24
TAU 24
50 kDa
37 kDa
25 kDa
B
BHT 24
TAU 24
C
Cruzipain Activity
O.D (a.u)
40000
30000
20000
10000
0
**
BHT
TAU

Figure S2. Induction of autophagy promotes cruzipain activation at early times. (**A**) Western blot analysis of cruzipain in total protein extracts from epimastigotes exposed to *in vitro* metacyclogenesis. Samples were collected after 24 h and lysates were obtained. The different forms of cruzipain were detected with a polyclonal antibody against this protein. (**B**) Enzyme assay of total protein extracts from epimastigotes exposed to *in vitro* metacyclogenesis. Samples were collected at 24 h to obtain lysates for gel zymography. (**C**) Quantification of cruzipain activity by OD of the bands. Images are representative of two independent experiments.